THE DESIGN AND TESTING OF TIME-VARYING INDUCTORS AND CAPACITORS FOR AN ELECTRICAL SPEECH SYNTHESIZER

by

KENNETH FREEMAN WICKWIRE

B.Eng.(Hons.), Nova Scotia Technical College, 1965

A THESIS SUBMITTED IN PARTIAL FULFILMENT OF THE REQUIREMENTS FOR THE DEGREE OF

MASTER OF APPLIED SCIENCE

in the Department of
Electrical Engineering

We accept this thesis as conforming to the required standard

Research Supervisor

Members of the Committee

Head of the Department

Members of the Department
of Electrical Engineering

THE UNIVERSITY OF BRITISH COLUMBIA

December, 1967

In presenting this thesis in partial fulfilment of the requirements for an advanced degree at the University of British Columbia, I agree that the Library shall make it freely available for reference and study. I further agree that permission for extensive copying of this thesis for scholarly purposes may be granted by the Head of my Department or by his representatives. It is understood that copying or publication of this thesis for financial gain shall not be allowed without my written permission.

Department of Electrical Engineering
The University of British Columbia
Vancouver 8, Canada

Date Jan. 3, 1968

ABSTRACT

This thesis describes the design and testing of time-varying inductors and capacitors for use in an electrical analogue of the human vocal tract. The inductors and capacitors were varied in accordance with an external control signal by varying the value of a resistor in a circuit which used operational amplifiers to simulate a variable impedance. The inductor actually tested is not a true inductor, since its voltage e and current i are related by the equation $e(t) = L(t) \frac{di}{dt}$, where $L(t)$ is an externally controlled time function. A device for which $e(t) = L(t) \frac{di}{dt}$ will probably be adequate for use in a vocal tract analogue. A true inductor for which $e(t) = \frac{d}{dt} (L(t)\ i(t))$ can be realized by making a change in the circuit tested. For the inductor tested, the maximum allowable input voltage and current are $\pm$ 2 volts and $\pm$ 2 ma, respectively. For the capacitor, the allowable ranges are $\pm$ 4 volts and $\pm$ 20 ma. The inductance and capacitance can be varied over a range of 250:1 with good linearity with respect to external control voltage and audio frequency. The inductor's Q exceeds 50 and the capacitor's Q exceeds 200 for all frequencies between 200 Hz and 5 KHz.

A system for routing control signals from a digital computer to the vocal tract analogue has been devised. Each component in the analogue is to be serviced by the computer at discrete time intervals. Between computer service times, the value of each component is interpolated by the up-down counter-digital comparator interpolating system described in the thesis.

TABLE OF CONTENTS

Page

LIST OF ILLUSTRATIONS

ACKNOWLEDGEMENT

The author would like to thank Dr. R.W. Donaldson for his help and guidance throughout this research project and Professor F.K. Bowers for reading the thesis. The author is also indebted to the graduate students who proofread the thesis and especially to Mrs. M. Wein who typed it.

The author also wishes to express his gratitude to the National Research Council of Canada for a Bursary in 1965 and to the University of British Columbia for a Graduate Fellowship in 1966.

1. INTRODUCTION

1.1 Potential Uses of Speech Synthesizers

This thesis describes the design and testing of time-varying inductors and capacitors for an electrical speech synthesizer. A speech synthesizer would be useful as an output for a computer, a language translation system, a reading machine for the blind, and a communication system which encodes and transmits speech in phonemic units.[1,2] Such a communication system would have to transmit approximately 20 bits per second, as compared with the 20 or more kilobits per second transmitted by conventional voice communication systems. A speech synthesizer would be useful for research on linguistics and as a clinical aid for speech therapy. The knowledge gained in developing a synthesizer would be of use to those working on automatic speech recognition.

1.2 Previous Research on Speech Synthesis

Speech synthesizers may be divided into two categories: terminal analogues and vocal tract analogues.

A terminal analogue synthesizer attempts to produce an acoustic signal whose short-time Fourier transform duplicates that of the desired speech signal. The first successful terminal analogue synthesizer was the Vocoder in 1936.[3,4] It produced connected speech; however, this speech lacked naturalness. Further research has improved the quality of the speech output.[5] At present, a computer controlled terminal analogue is being developed at the Massachusetts Institute of Technology.[6,7]

A vocal tract analogue attempts to produce speech by simulating the human vocal tract. The pressure and air velocity relationships of the vocal tract can be simulated by a time-varying non-uniform transmission line.[8,9] Static electrical analogues [9,10] which produce vowels and certain consonants have been built, but these analogues do not produce connected speech. A time-varying electrical analogue which synthesized certain vowel-consonant and consonant-vowel sequences was built by Rosen,[11,12] however, limitations of his system for controlling the analogue made it difficult to synthesize longer phoneme sequences.[13,14] The work described in this thesis is the beginning of an effort to synthesize speech by controlling the components of an electrical analogue of the human vocal tract by a high-speed digital computer.

The principal components of the analogue are time-varying inductors and capacitors whose inductance and capacitance vary in accordance with an external control signal. There are devices which simulate time-invariant inductance and capacitance,[15,16,17] but to the author's knowledge, only Rosen [11,12] has built inductors and capacitors whose time-variation is controlled by an external voltage. For his inductor Rosen used a saturable reactor. For his capacitor he used a variable-gain amplifier with a capacitor in the feedback path. In the saturable reactor the inductance is controlled by using an auxiliary winding to control the degree of saturation in an iron core. The auxiliary winding requires a non-linear current driver to compensate for the non-linearity of saturation in the iron. The capacitor used by Rosen is undesireable because a high supply voltage is required to

prevent input voltages in excess of one volt from saturating the amplifier when its gain is high.

1.3 Scope of this Thesis

This thesis describes the design and testing of a time-varying inductor and capacitor. The time-variation depends on an external time-varying control voltage. Although the inductor and capacitor are for use in an electrical analogue of the human vocal tract, they are not restricted to this context.

The inductor actually tested is not a true time-varying inductor, since the voltage e and the current i are related by the equation $e(t) = L(t) \frac{di}{dt}$. As shown in Chapter III, a device for which $e(t) = L(t) \frac{di}{dt}$ will probably be adequate for use in a vocal tract analogue. A true time-varying inductor for which $e(t) = \frac{d}{dt} (L(t)i(t))$ can be realized by making a minor change in the circuit tested.

The inductance and capacitance of the devices tested can be varied over a range which exceeds 250:1 with good linearity with respect to external control voltage and audio frequency. The maximum allowable input voltage and current is $\pm$ 2 volts and $\pm$ 2 ma for the inductor and $\pm$ 4 volts and $\pm$ 20 ma for the capacitor. The inductor's Q exceeds 50 and the capacitor's Q exceeds 200 for all frequencies between 200 Hz and 5000 Hz. The most expensive elements in the inductor and capacitor are the operational amplifiers; the inductor requires four and the capacitor, which has one terminal grounded, requires two. If both capacitor terminals are to be ungrounded, two additional operational amplifiers are required.

2. OPERATION AND SIMULATION OF THE HUMAN VOCAL MECHANISM

2.1 Description of the Vocal Mechanism

Speech is produced by controlled movements of the vocal mechanism. This mechanism, shown in cross-section in Fig. 2.1, consists basically of the lungs, trachea, vocal cords, vocal tract, and nasal tract.

The lungs, trachea and vocal cords provide an air velocity source for the vocal tract. The slit-like orifice between the vocal cords is the glottis. The instantaneous velocity of the air passing through the glottis is approximately proportional to the area of the glottal opening, independent of the shape of the vocal and nasal tracts.

The vocal tract is a tube which is non-uniform in cross-sectional area. It begins at the vocal cords and terminates at the lips. The tract of an adult male is approximately 17 cm. long. The forward portion of the tract may be varied in cross-sectional area from zero to approximately 20 cm^2. The variation in cross-sectional area of the tract near the glottis is very small. In the region near the mouth, the length of the tract also varies during speech production.

The nasal tract is similar to the vocal tract, except that its cross-sectional area is fixed. For an adult male the nasal tract is approximately 12 cm. long and has a volume of approximately 60 cc. The degree of coupling between the vocal and nasal tracts is controlled by the size of the opening at the velum.

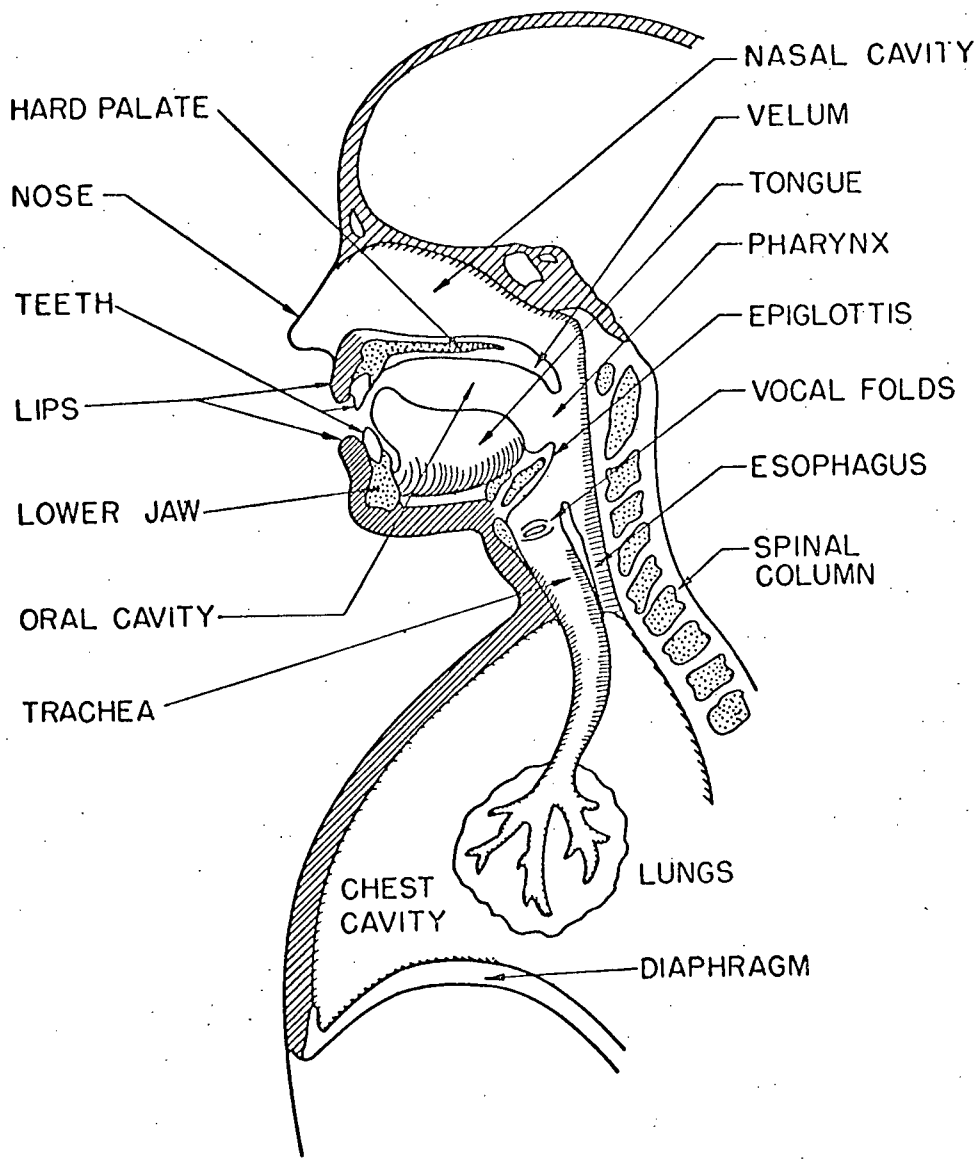

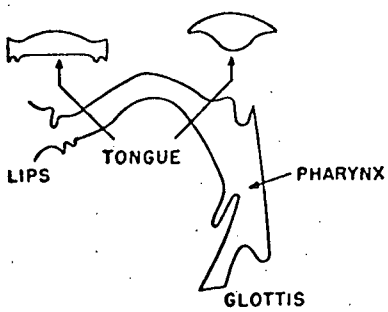

Boundaries of the vocal tract during the production of the vowel [e]. A midsagittal section and two transverse sections are shown (from T. Chiba and M. Kajiyama [13]).

Fig. 2.1. Diagram of the human vocal mechanism based on a midsagittal section.

The glottis is the primary source of excitation. In voiced sounds, it opens and closes at the rate of approximately 125 Hz. In unvoiced sounds, air is blown through the glottis which, in this case, remains open and does not vibrate.

Secondary sources of excitation may appear within the vocal tract. They may result from turbulence created by a narrow constriction in the tract or by a closure followed by a sudden release of air.

2.2 The Basic Speech Sounds [19]

The basic unit of speech is the phoneme. Phonemes are classified according to their manner and place of production in the vocal tract. The approximate vocal tract configurations for the principal English phonemes appear in Fig. 2.2.

During the production of vowels, the vocal tract remains in a relatively fixed configuration with no nasal coupling. All vowels are voiced, and the air flow through the vocal tract is non-turbulent.

The consonants include all other phonemes except diphthongs and affricates, which are combinations of vowels and consonants.

Fricative consonants are produced by a constriction which causes air turbulence in the vocal tract. They may be either voiced or unvoiced.

Stop consonants are produced by the sudden release of pressure built up behind a complete closure at some point in the vocal tract. They may be either voiced or unvoiced.

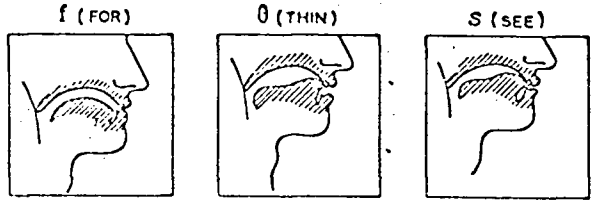

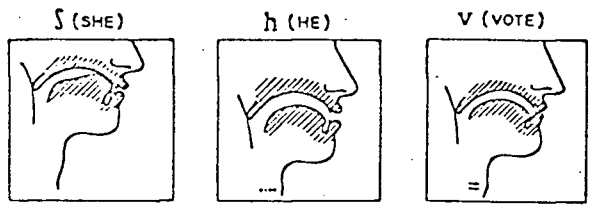

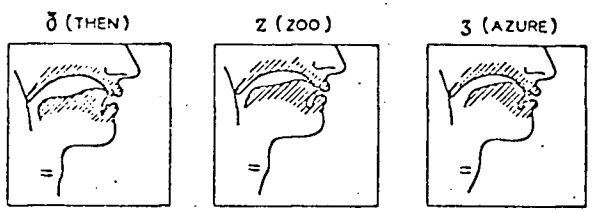

Vocal tract profiles for the fricative consonants of English. The short pairs of lines drawn on the throat represent vocal cord operation (adapted from POTTER, KOPP and GREEN)

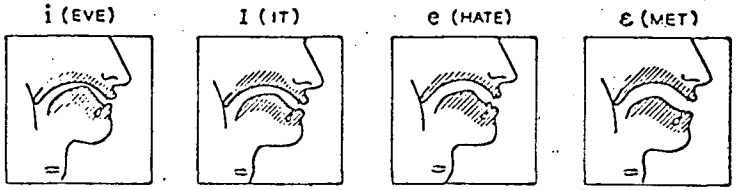

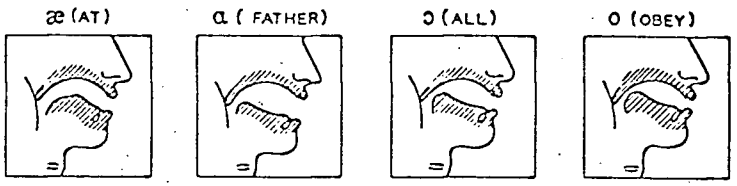

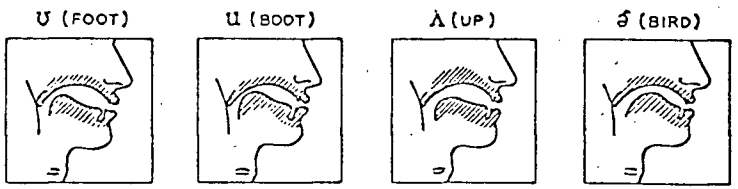

Schematic vocal tract profiles for the production of English vowels (adapted from POTTER, KOPP and GREEN)

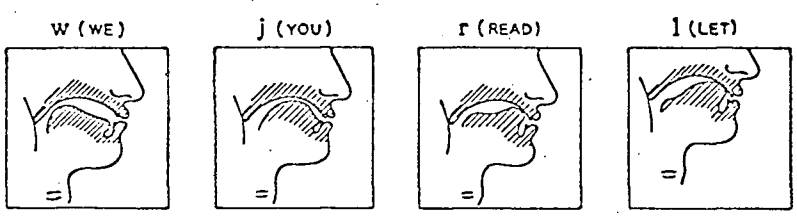

Vocal tract configurations for the beginning positions of the glides and semivowels (after POTTER, KOPP and GREEN)

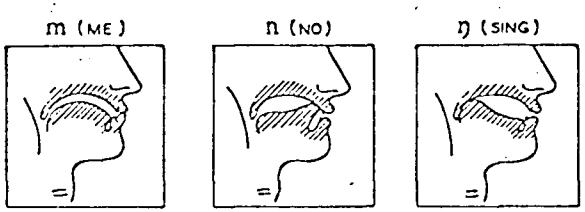

Vocal profiles for the nasal consonants (after POTTER, KOPP and GREEN)

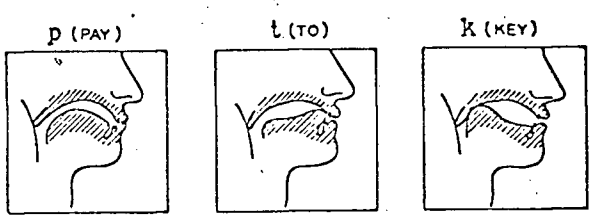

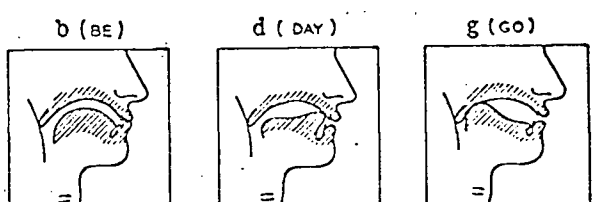

Articulatory profiles for the English stop consonants (after POTTER, KOPP and GREEN)

Fig. 2.2 Vocal Tract Profiles for the Principle Phonemes in the English Language [20]

Nasal consonants, which are voiced, are produced when the front portion of the vocal tract is closed and the velum is opened. In this case, air passes along the nasal tract and out through the nostrils.

Glides and semivowels are similar to vowels and are voiced. Glides are dynamic sounds which result from movement of the vocal tract towards or away from a vowel configuration. The oral channel is more constricted in the semivowels than in vowels, and the tongue tip is up.

The diphthongs and affricates are combination sounds. The diphthong is a combination of two vowel sounds, and the affricate is a combination of a stop and fricative consonant.

2.3 An Electrical Analogue of the Vocal Mechanism

All speech sounds depend on the vocal tract configuration, glottal excitation and degree of coupling with the nasal tract. By making an electronic analogue of the vocal tract and by controlling the analogue by a digital computer, it should be possible to synthesize connected speech.

The vocal tract may be approximated as a cascade of short right circular cylinders [8,9]. Two electrical analogues for a cylinder who's length ℓ is much less than the highest sound wave-length, appear in Fig. 2.3. Voltage is analogous to pressure and current to volume velocity. Inductance L is analogous to the inertance of the air mass. Capacitance C is analogous to the compliance of the air volume. The resistance R represents the power dissipated in viscous friction at the tube wall, and the conductance

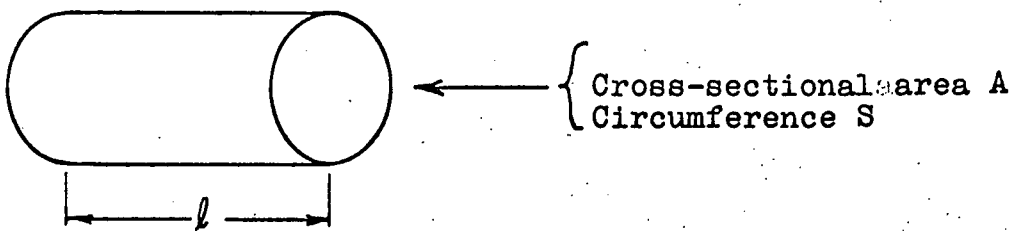

Right-Circular Cylinder

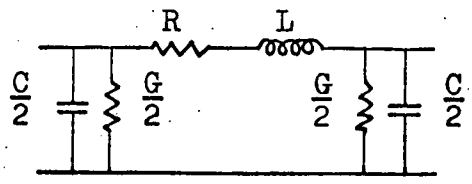

π section

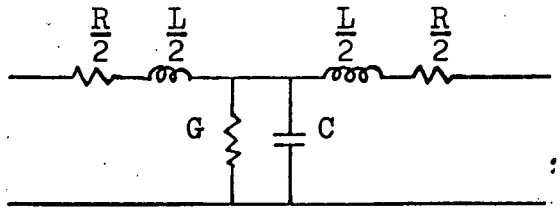

T section

$$L = \frac{\rho \ell}{A}$$

$$R = \frac{S \ell}{A^2} \sqrt{\frac{\omega \rho \mu}{2}}$$

$$C = \frac{A \ell}{\rho c^2}$$

$$G = \frac{S(\eta - 1)}{\rho c^2} \ell \sqrt{\frac{\lambda \omega}{2 C_p \rho}}$$

ρ = air density
μ = viscosity coefficient of air
ω = radian frequency
C_p = specific heat of air at constant pressure

c = speed of sound in air
η = adiabatic constant of air
λ = coefficient of heat conduction

Fig. 2.3 Electrical Analogues of a Short Cylinder

G represents the power loss due to heat conduction at the tube wall. In the vocal tract, $R/\omega L$ and $G/\omega C$ are small for the frequencies of interest and R and G may be neglected.

An analogue of the vocal tract is obtained by cascading T or π sections corresponding to adjacent cylinders, as shown in Fig. 2.4.

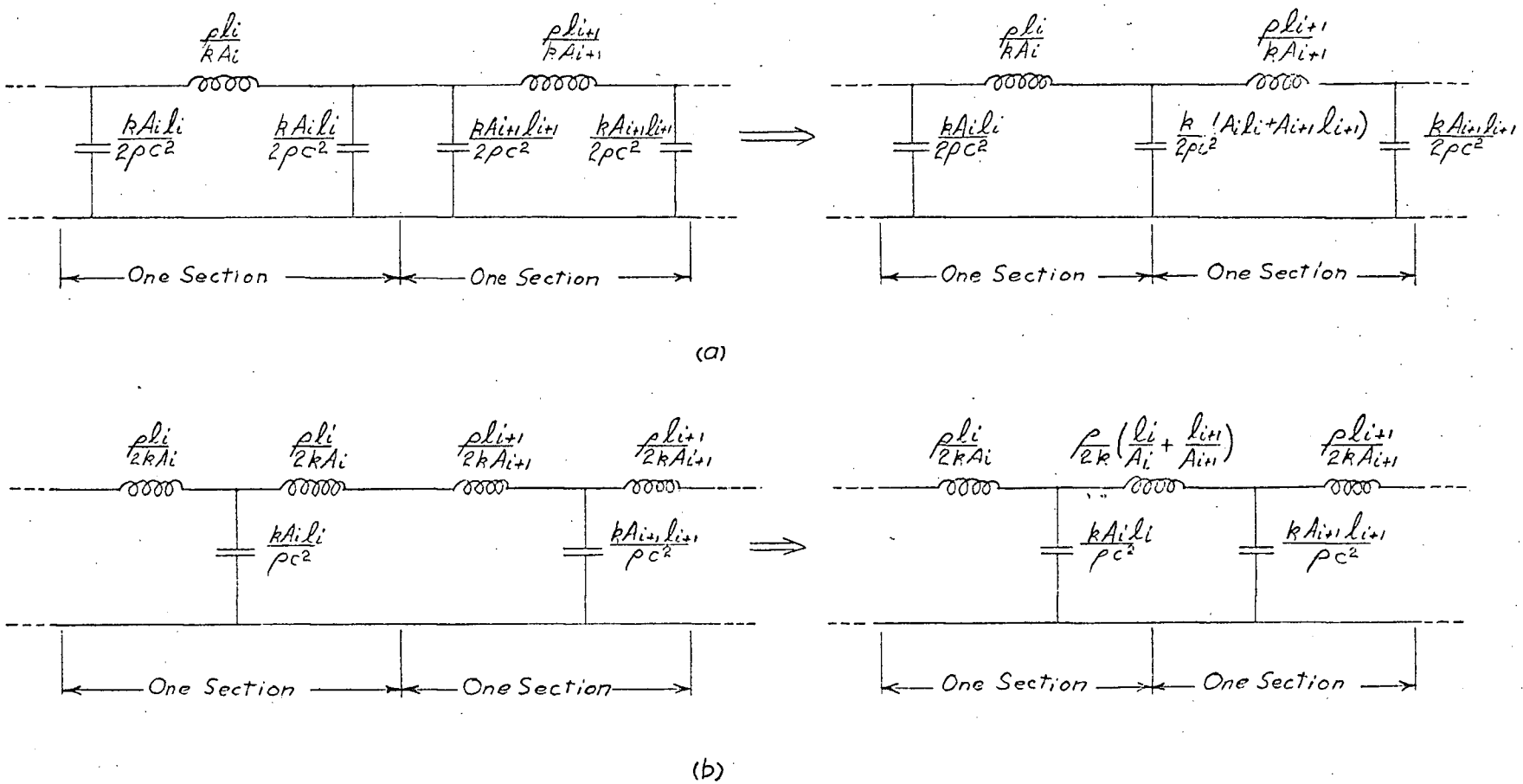

Fig. 2.4 Models of Cascaded Right Circular Cylinders

(a) π sections; separate and combined (b) T sections; separate and combined

Constant k is an arbitrary constant which is chosen to make the L and C correspond to practical electrical values.

Since the cross-sectional area of most of the nasal passage is constant, it is simulated mainly by fixed components (see Fig. 2.5). The degree of coupling to the vocal tract depends on the variable inductor and capacitor nearest the junction of the nasal stub and the vocal tract.

The glottis acts as an air velocity source, the velocity being proportional to the area of the glottal opening. In the analogue the glottis becomes a current source whose current $i(t) = A(t) \sqrt{2Pso/\rho}$. Constant Pso is the mean value of the sub-glottal pressure and A(t) is the area of the glottal opening. To simulate turbulance or a sudden release of pressure which follows a closure, a voltage source is placed in series with one of the ungrounded inductors in the analogue. In simulating turbulance the voltage source is a white noise source. A suddenly applied decaying exponential of the form $v(t) = E\, e^{-\frac{t}{\tau}}$ is used to simulate closure followed by release.

To a first approximation, the mouth and nostrils appear to the vocal tract as plane vibrating surfaces, all parts of which move in phase. The radiating element is set in a baffle that is the head. To the analogue, the mouth and nostrils appear as a large constant resistor in parallel with a small inductor whose inductance is $k\rho / \sqrt{\pi A}$. Scale factor k is identical to the scale factor in Fig. 2.4 and A is the cross-sectional area of the mouth or nose opening.

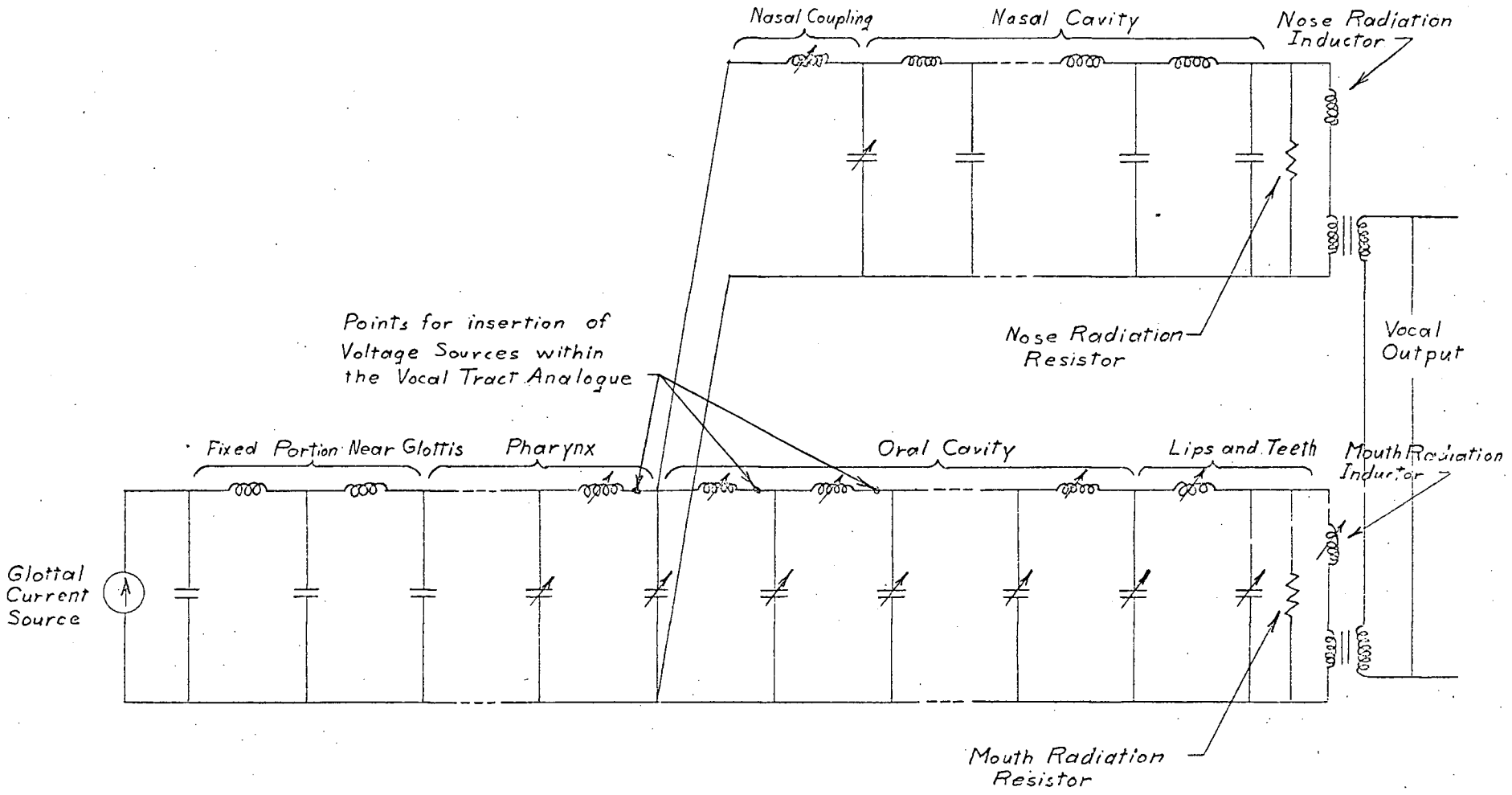

Fig. 2.5 Electrical Analogue of the Human Vocal Tract. Inductors, Capacitors and Excitation Voltage and Current Sources are to be Controlled by a Digital Computer

3. SIMULATION OF TIME-VARYING INDUCTORS AND CAPACITORS

3.1 Requirements for the Reactive Elements

The instantaneous inductance L of a two-terminal device is defined as the ratio of the flux linkages λ of the device to the current i passing through the device. The voltage e across the device is equal to the time derivative of the flux linkages. The instantaneous capacitance C of a two terminal device is defined as the ratio of the charge q contained in the device to the voltage e across the two terminals. The current passing through the device is equal to the time derivative of the stored charge. The similarity between these two definitions is indicated in Fig. 3.1.

The specification for the inductor and capacitor were decided upon after considering a previous work by Rosen,[11] and after deciding that solid state circuitry would be used. As a result of tests on a static vocal tract analogue, Rosen,[11] found that the maximum length of a cylinder section should be 1.5 cm. Satisfactory vowels have been produced by using only an area ratio of 29:1, but it was decided to have a full range of 250:1 in the dynamic analogue. This means that the inductors and capacitors must vary over a 250:1 range. The Q (quality factor) of the reactive elements was chosen to be greater than 50. Rosen[11] showed that a Q equal to or greater than 30 was adequate. The Q can always be reduced by placing resistors in series with the inductors and in parallel with the capacitors. Because of the large dynamic signal range expected in the vocal tract analogue, it was decided that the maximum allowable input voltage and current at the terminals of the reactive

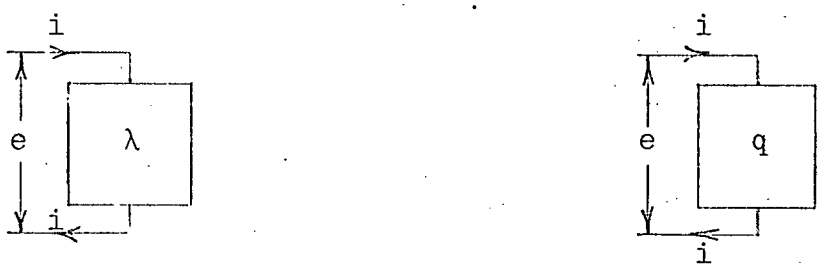

$L \equiv \frac{\lambda}{i}$ $\qquad$ $C \equiv \frac{q}{e}$

$\lambda = Li$ $\qquad$ $q = Ce$

$$e = \frac{d\lambda}{dt} = \frac{d(Li)}{dt} = L\frac{di}{dt} + i\frac{dL}{dt} \qquad i = \frac{dq}{dt} = \frac{d(Ce)}{dt} = C\frac{de}{dt} + e\frac{dC}{dt}$$

Inductance $\qquad$ Capacitance

Fig. 3.1 Voltage-Current Relations for Time-Varying Capacitors and Inductors

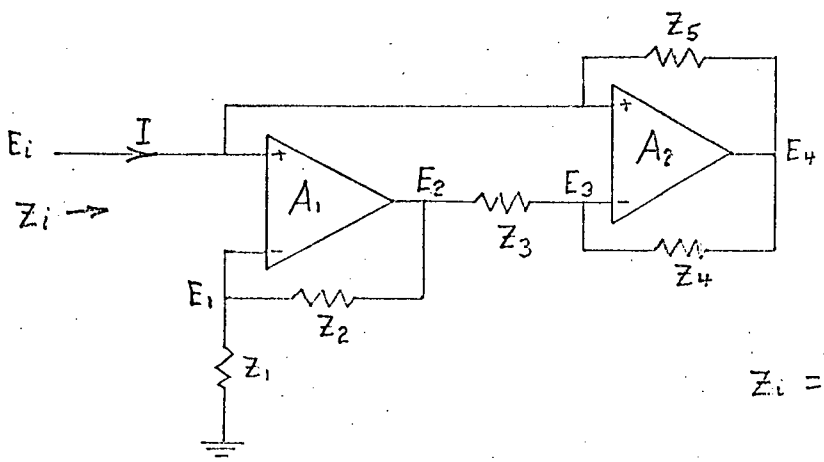

$$Z_i = \frac{Z_1 Z_3 Z_5}{Z_2 Z_4}$$

Fig. 3.2 Riordan's Circuit for Simulation of Impedance [21]

elements should be as large as possible subject to the constraint that standard solid state components be used to realize these elements. Initial experiments showed that if 15 volt operational amplifiers were used, the input voltage could be as large as $\pm$ 2 volts for both the inductor and capacitor. The maximum input current was $\pm$ 2 ma for the inductor and $\pm$ 20 ma for the capacitor.

3.2 The Time-Varying Inductor

3.2.1 Steady State Analysis

Many circuits for simulating time-invariant inductors have been considered, [15,16,17] but none of these could be extended to the simulation of time-varying inductors. The required range of inductance or the required Q could not be realized, or the maximum input voltage and current were too small. The basic circuit finally chosen was one used by Riordan [21] to produce an adjustable time-invariant inductor. Experimentation showed that the inductance range of 250:1 could be realized by varying only one resistor. Riordan's circuit appears in Fig. 3.2. Assuming that the current into the amplifier inputs is negligible, and that $A_1 >> 1$ and $A_2 >> 1$, it can be shown that

$$E_4 = E_i \left(1 - \frac{Z_2 Z_4}{Z_1 Z_3}\right) \tag{3.2}$$

The input current I is the current in Z_5, so that

$$Z_i = \frac{E_i}{I} = \frac{Z_1 Z_3 Z_5}{Z_2 Z_4} \tag{3.3}$$

If either Z_2 or Z_4 is a capacitor and if the remaining Z's are

resistors, then the input impedance is inductive.

$$Z_i = s\,\frac{C_2R_1R_3R_5}{R_4} = sL$$

This circuit, as it stands, is not suitable for use in a vocal tract analogue because one input terminal is grounded. To obtain an ungrounded inductor, two identical circuits are placed in the back-to-back configuration of Fig. 3.3.

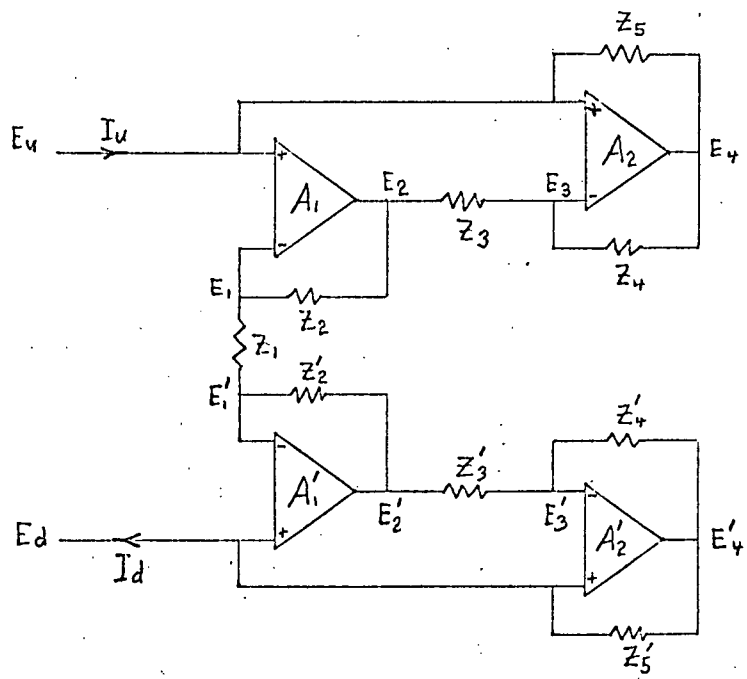

Fig. 3.3 Simulation of an Ungrounded Impedance

Analysis of the circuit in Fig. 3.3 is similar to that of the grounded inductor, in Fig. 3.2

$$E_1 = E_3 = E_u$$

and

$$E_1' = E_3' = E_d$$

$$E_2 = E_u + \frac{Z_2}{Z_1}(E_u - E_d), \tag{3.4}$$

$$E_4 = E_u - \frac{Z_2 Z_4}{Z_1 Z_3}(E_u - E_d)$$

and

$$I_u = \frac{Z_2 Z_4}{Z_1 Z_3 Z_5}(E_u - E_d)$$

Similarly

$$I_d = \frac{Z_2' Z_4'}{Z_1 Z_3' Z_5'}(E_u - E_d)$$

Let

$$Z = \frac{Z_1 Z_3 Z_5}{Z_2 Z_4}$$

and

$$Z' = \frac{Z_1 Z_3' Z_5'}{Z_2' Z_4'}$$

Then

$$I_u = \frac{(E_u - E_d)}{Z} \tag{3.5}$$

and

$$I_d = \frac{(E_u - E_d)}{Z'} \tag{3.5}$$

Equations 3.5 and 3.6 suggest the circuit model of Fig. 3.4a. Note that current $\Delta I = I_u - I_d$ results from a mismatch between Z and Z'. If $Y = \frac{1}{Z}$ and $Y' = \frac{1}{Z'}$, then Fig. 3.4b becomes the Norton equivalent of Fig. 3.4a. Let

$$Y = Y' + \Delta Y$$

Then

$$YE_d = Y'E_d + \Delta Y E_d.$$

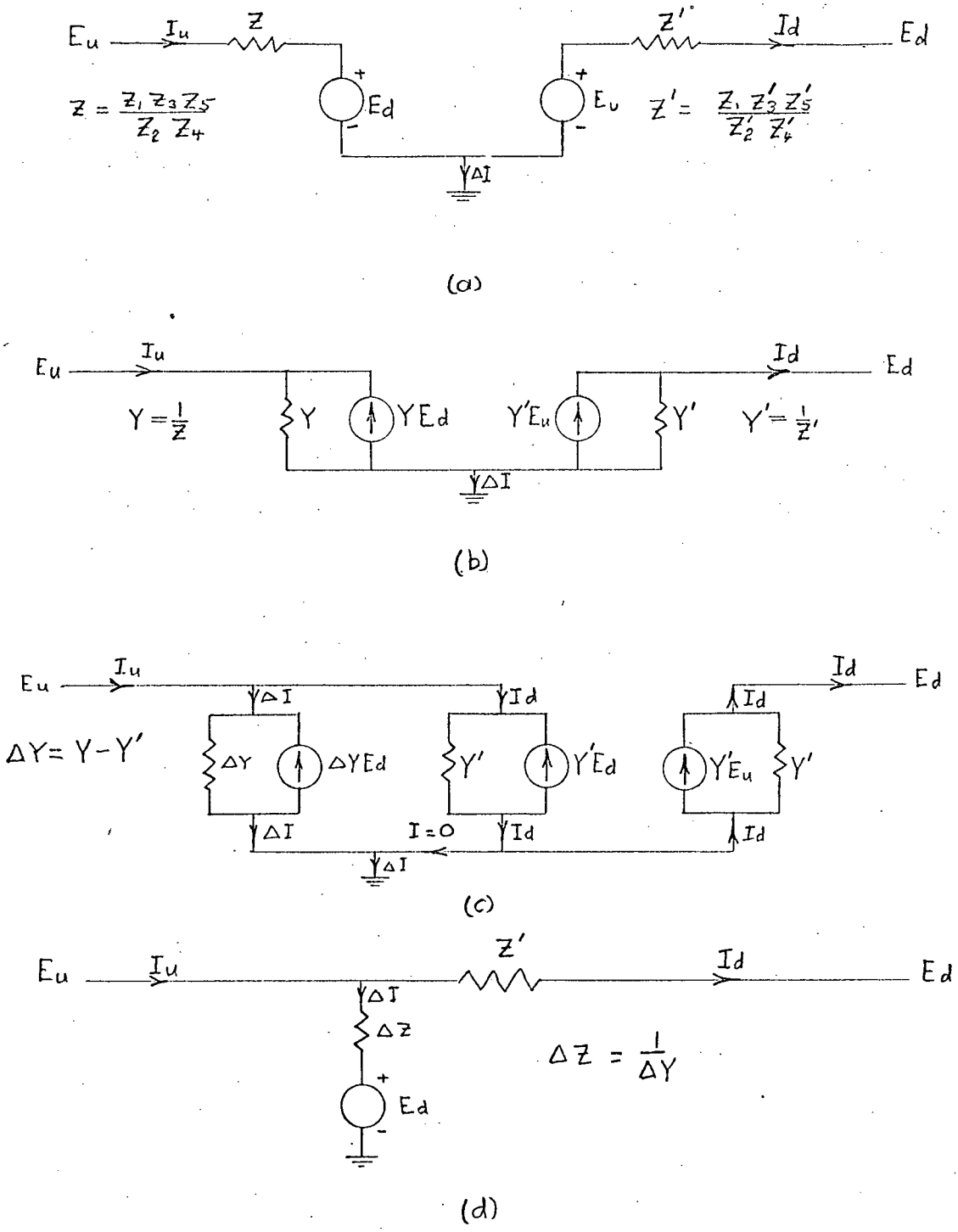

Fig. 3.4 Circuit Models for the Ungrounded Impedance in Fig. 3.3

The circuit model appears as in Fig. 3.4c. Further rearrangements result in the model in Fig. 3.4d, where

$$\Delta Z = \frac{1}{\Delta Y}$$

Therefore

$$\Delta Z = Z_1 \frac{Z_3 Z_3' Z_4 Z_4'}{Z_2 Z_3' Z_4 Z_5' - Z_2' Z_3 Z_4' Z_5} \qquad (3.7)$$

Equation 3.7 shows that the larger the mismatch between $Z_2 Z_3' Z_4 Z_5'$, and $Z_2' Z_3 Z_4' Z_5$, the smaller the magnitude of ΔZ. Therefore, Z_1 is chosen to be the variable resistor, and $Z_2 Z_3' Z_4 Z_5'$ is matched as closely as possible to $Z_2' Z_3 Z_4' Z_5$. If Z_2 and Z_2' in Fig. 3.3 are capacitors and all other impedances are resistors, then the resulting ungrounded inductor can be modelled as in Fig. 3.5.

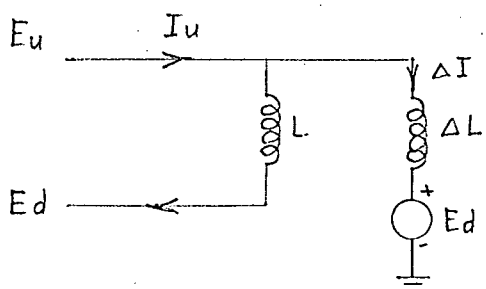

$$L = \frac{C_2 R_1 R_3 R_5}{R_4}$$

$$\Delta L = R_1 \frac{R_3 R_3' R_5 R_5' C_2 C_2'}{(C_2' R_3' R_4 R_5' - C_2 R_3 R_4' R_5)}$$

Fig. 3.5 Circuit Model for the Ungrounded Inductor

3.2.2 Transient Analysis

If Z_1 in Fig. 3.1 is a time-varying resistor, $R_1(t)$, and Z_2 a capacitor, the circuit does not behave as a true time-varying inductor.

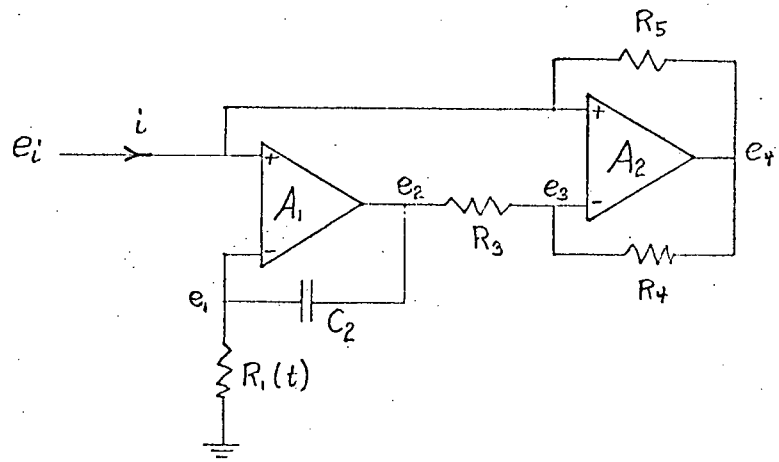

Fig. 3.6 Circuit for which $e(t)=L(t)\frac{di}{dt}$. $L(t)=R_1(t)\frac{C_2R_3R_5}{R_4}$

If the circuit in Fig. 3.6 is at rest for $t = -\infty$, then the input current i is

$$i = \frac{R_4}{C_2R_3R_5}\int_{-\infty}^{t}\frac{e_i}{R_1(t)}\,dt$$

Differentiation and rearrangement gives

$$e_i = L(t)\frac{di}{dt}, \tag{3.10}$$

where

$$L(t) = R_1(t)\frac{C_2R_3R_5}{R_4} \tag{3.11}$$

Equations 3.10 and 3.11 also apply to the circuit in Fig. 3.3, provided $Z_1 = R_1(t)$, $Z_2 = Z_2' = C_2$, $Z_3 = Z_3' = R_3$, $Z_4 = Z_4' = R_4$ and

and $Z_5 = Z_5' = R_5$.

A true ungrounded time-varying inductor is realized if either R_3 and R_3' or R_5 and R_5', rather than R_1, are varied simultaneously. More circuitry is required to vary R_3 and R_3' or R_5 and R_5', and considerable mismatch caused by loss in synchronization between resistor pairs could result.

In eqn. 3.10 the term $i \frac{dL}{dt}$ is absent. In the vocal tract analogue, this term is proportional to the rate of change of A/ℓ. The term $L \frac{di}{dt}$ depends on the rate of change of inductor current. If $i(t) = I \cos(\omega t + \phi)$, then $\left| L \frac{di}{dt} \right| = \left| I\omega\rho\ell / kA \right|$,

$$\left| i \frac{dL}{dt} \right| = \left| \frac{I\rho}{k} \left(\frac{\ell}{A}\right)^2 \frac{d(A/\ell)}{dt} \right|, \text{ and } \left| i \frac{dL}{dt} \right| \Big/ \left| L \frac{di}{dt} \right| = \left| \frac{\ell}{\omega A} \frac{d(A/\ell)}{dt} \right|.$$

In the human vocal tract, the term $\left| \frac{\ell}{\omega A} \frac{d(A/\ell)}{dt} \right| << 1$, except when the area A changes suddenly. A sudden change occurs, for example, in moving from a vowel to a stop consonant. Such changes occur between phonemes, and are present for only a few milliseconds. It is believed that the intelligibility of synthesized speech will not be noticably impaired by using inductors for which $e = L(t) \frac{di}{dt}$.

3.3 The Variable Capacitor

The variable capacitor was made from the same basic circuit as the inductor. The capacitor has the advantage that in the analogue one terminal is grounded. As before, the equation for the input impedance is eqn. 3.3. Laboratory experiments showed that it was best to choose Z_5 as the capacitor, Z_1 as the variable $R_1(t)$, and the remaining impedances as fixed resistors, as shown in Fig. 3.7.

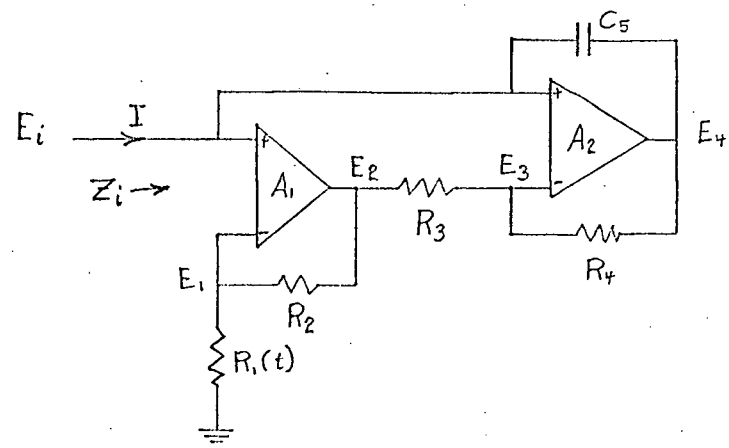

Fig. 3.7 Time-Varying Capacitor

If R_1 is a function of time, the capacitor behaves as a true time-varying capacitor. In analyzing the circuit, consider the ratio $\frac{e_4}{e_i}$ when the capacitor C_5 is removed. Because the components are all resistors, eqn. 3.2 can be used directly to give

$$e_4 = e_i \left(1 - \frac{R_2 R_4}{R_1(t) R_3}\right) \tag{3.12}$$

A model for eqn. 3.12 is shown in Fig. 3.8, where

$$i = C_5 \frac{d(Ke_i)}{dt} = \frac{d(Ce_i)}{dt}$$

$$C(t) = K(t)C_5 = \frac{C_5 R_2 R_4}{R_1(t) R_3} \cdot \tag{3.13}$$

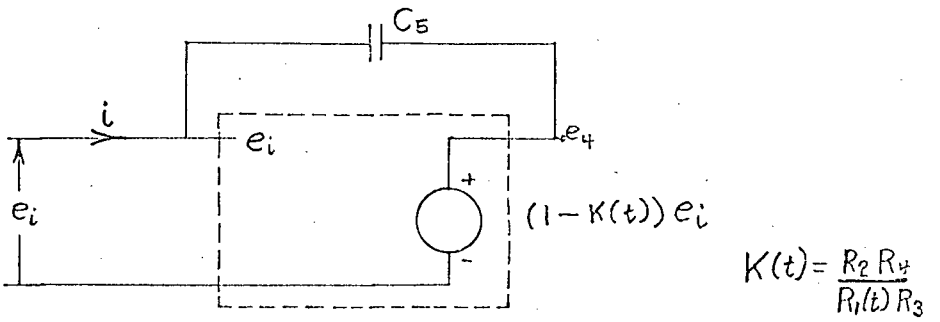

Fig. 3.8 Circuit Model for Equation 3.12

The equations for the vocal tract analogue in Fig. 2.3 show that the inductance is inversely proportional to A/ℓ and the capacitance is directly proportional to $A\ell$. If R_1 is inversely proportional to A/ℓ then

$$L = \frac{K_L}{A/\ell} \quad \frac{C_2R_3R_5}{R_4} \qquad \text{for } R_1 = \frac{K_L}{A/\ell}$$

where K_L is a constant. If C is proportional to $A\ell$

$$C = \frac{C_5R_2R_4}{R_3} \quad \frac{A\ell}{K_C} \qquad \text{for } R_1 = \frac{K_C}{A\ell}$$

where K_C is constant. It will be seen in Chapter 4 that because C is proportional to A, and L is inversely proportional to A, the control of the vocal tract analogue is simplified, when the lengths ℓ of adjacent sections in Fig. 2.4 are constant and equal.

4. CONTROL OF THE VOCAL TRACT ANALOGUE

4.1 Overall Plan for Controlling the Inductors and Capacitors

The vocal tract analogue is to be a cascade of L-C sections which simulate cylinders of length ℓ and time-varying cross-sectional area A(t), as shown in Fig. 2.5. It follows from Fig. 2.4 that for each section the product $LC = \ell^2/c^2$ must be maintained.

During speech production the cross-sectional area at each point along the vocal tract changes with time. In the electrical analogue, the control of the components is to be by digital computer. It is desirable to minimize the number of times per second that the computer services the analogue. The computer will then be able to devote more of its time to calculating the required parameter settings from stored phoneme sequences. To reduce the number of computer service calls required, an interpolating system was built. Between service calls, this interpolating system causes each reactive element to vary with time in a stepwise fashion, as shown in Fig. 4.1 for a capacitor.

The interpolating system makes stepwise approximations of straight lines which are used for piecewise linear approximations of curves. It is desireable to use the analogue as a static analogue as well as a dynamic one. For this reason the interpolating system was designed to make a reactive element move towards a specified value and then remain there until a new value was specified.

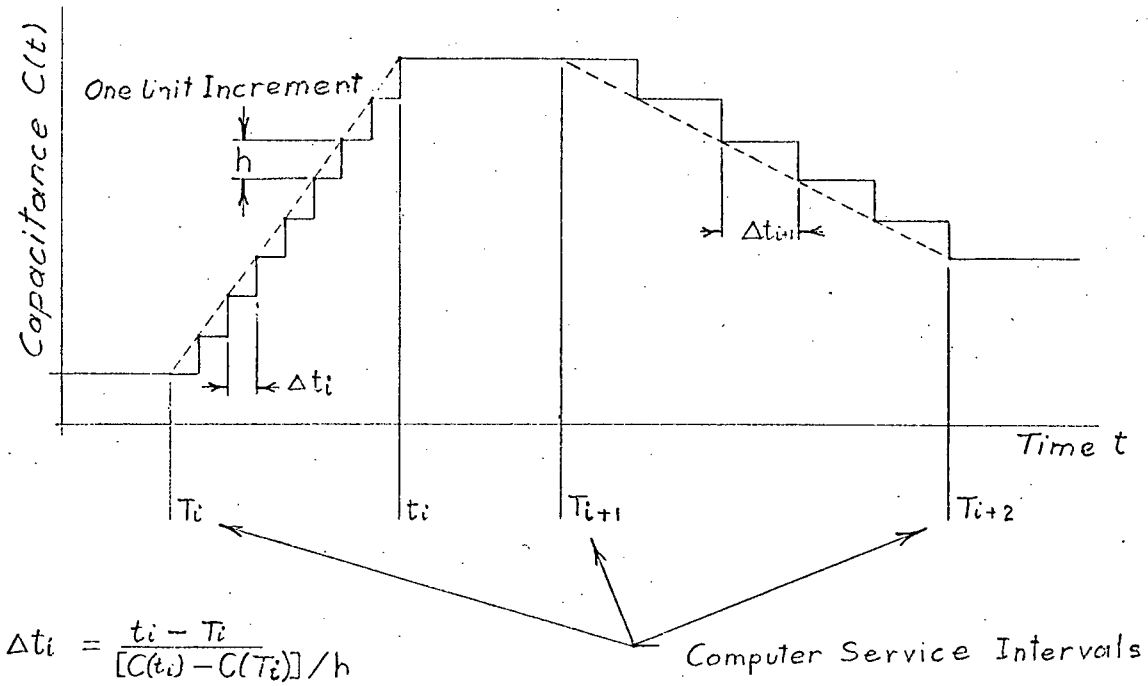

Fig. 4.1 Illustrating the effect of the interpolating system

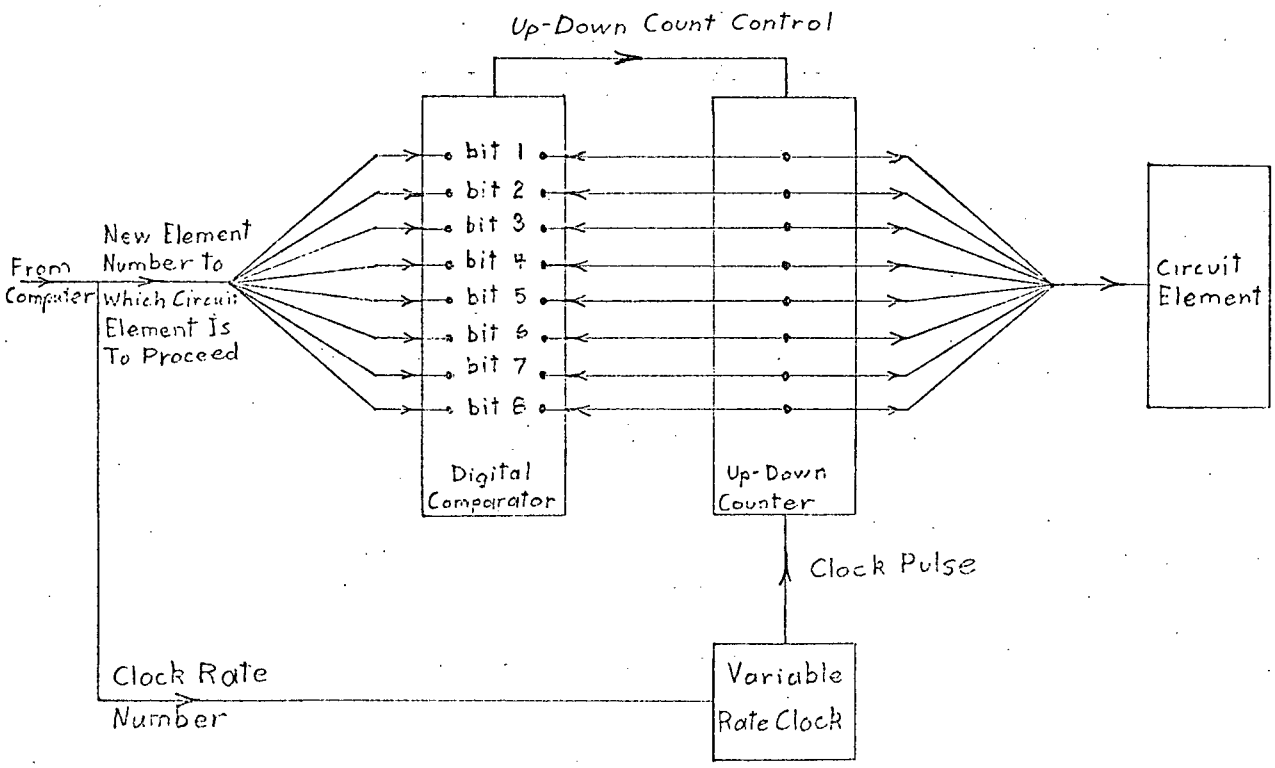

Fig. 4.2 Block Diagram of the Interpolating System

During each service call, the computer will deliver to the element serviced an eighteen bit binary number. Eight bits of this number will specify the new value towards which the element is to proceed. Ten bits will specify the rate $1/\Delta t$ at which the element is to proceed to its new value. For sections where both A and ℓ vary, the computer will control the inductors and capacitors separately. For sections where ℓ is constant and only A varies it will be shown that the control can be simplified.

4.2 System Components for Control of the Inductors and Capacitors

An inductor or capacitor whose instantaneous value depends on a binary number can be made to move towards a specified value such as $C(t_i)$ in Fig. 4.1 with the aid of the digital comparator and an up-down counter. In Fig. 4.2, the reactive element's value depends on the binary number in the counter. The same binary number is also stored in one side of the digital comparator. The new binary number towards which the inductor or capacitor is to proceed is placed in the memory of the other side of the comparator. The digital comparator compares the new number with the number in the up-down counter. If the new number is larger, then the digital comparator tells the up-down counter to count up, until the number in the up-down counter equals the new number. If the new number is smaller, the up-down counter counts down. The rate at which the counter counts depends on the computer-controlled clock rate.

When the lengths ℓ_i and ℓ_{i+1} of two adjacent π sections in Fig. 2.4a are constant and equal, the combined capacitance C_π

between these sections is

$$C_\pi = \frac{k\,\ell}{\rho\, C^2}\left(\frac{A_i + A_{i+1}}{2}\right)$$

Although the inductors L_i and L_{i+1} must be controlled independently, the constraint $LC = \ell^2/C^2$ is maintained by controlling the capacitor C_π between the two adjacent sections with the average of the instantaneous value of the binary number for the two adjacent inductors, as shown in Fig. 4.3a.

When ℓ_i and ℓ_{i+1} in Fig. 2.4b are constant and equal, the combined inductance L_T between these sections is

$$L_T = \frac{\rho\ell}{k}\,\frac{1}{2}\left(\frac{1}{A_i} + \frac{1}{A_{i+1}}\right) = \frac{\rho\ell}{k}\left[2A_iA_{i+1}/(A_i+A_{i+1})\right]$$

Although the capacitors C_i and C_{i+1} must be controlled independently, the constraint $LC = \ell^2/C^2$ is maintained by controlling the inductor between two adjacent sections with the average of the instantaneous value of the binary number for the two adjacent capacitors as shown in Fig. 4.3b.

The control number for the combined inductance should be proportional to $2A_iA_{i+1}/(A_i+A_{i+1})$. A device which averages A_i and A_{i+1} will approximate the control number with $(A_i + A_{i+1})/2$. For control numbers differing by small ratios, the two quantities are almost equal. The error is 12.5% for an area ratio A_{i+1}/A_i of 2. The control number for the combined capacitance which is proportional to $(A_i+A_{i+1})/2$ is realized exactly using an averager. For this reason the scheme in Fig. 4.3a will be used in preference to the one in Fig. 4.3b.

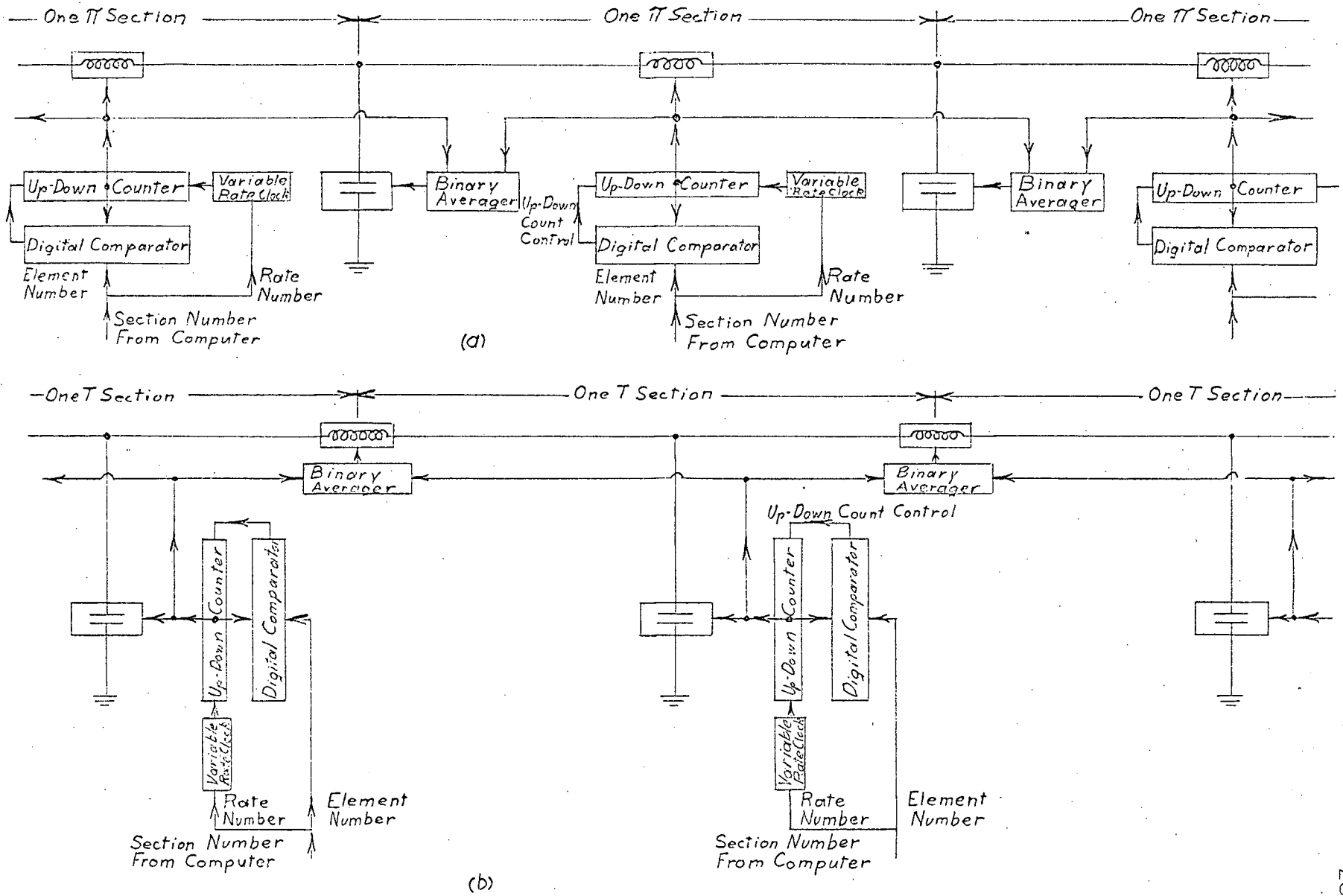

Fig. 4.3 Control of the Inductors and Capacitors (a) π sections
(b) T sections

4.3 The Digital Comparator

A block diagram of the digital comparator designed and tested is shown in Fig. 4.4. Fairchild μL-923 J-K flip-flops and Fairchild μL-914 dual two-input NOR gates were used in the actual circuit. Each digit X_k of the binary number $X = \sum_{k=0}^{n-1} 2^k X_k$ is compared with its corresponding digit Y_k of the binary number $Y = \sum_{k=0}^{n-1} 2^k Y_k$. A decision is first made as to whether X_{n-1} is larger than, smaller than, or equal to Y_{n-1}. If $X_{n-1} \neq Y_{n-1}$ then the up-down counter is instructed to count in the direction to make $X_{n-1} = Y_{n-1}$. When $X_{n-1} = Y_{n-1}$, X_{n-2} and Y_{n-2} are compared and the result determines whether the counter counts up, down, or remains unchanged. This process is repeated until X=Y.

The way in which the digital comparator was designed can be understood with the help of Fig. 4.5. The kth digit must have the truth table of Fig. 4.5, where U_k and D_k are the kth digits' decision that the counter must count up or down respectively. Control digit Z_{k-1} prevents comparison of less significant digits from influencing the counter until $X_k = Y_k$.

The truth table of Fig. 4.5 may be expressed in boolean form as follows:

$$U_k = Z_k \, X_k \, \overline{Y}_k$$

$$D_k = Z_k \, \overline{X}_k \, Y_k$$

$$Z_{k-1} = Z_k \, \overline{U_k} \, \overline{D_k}$$

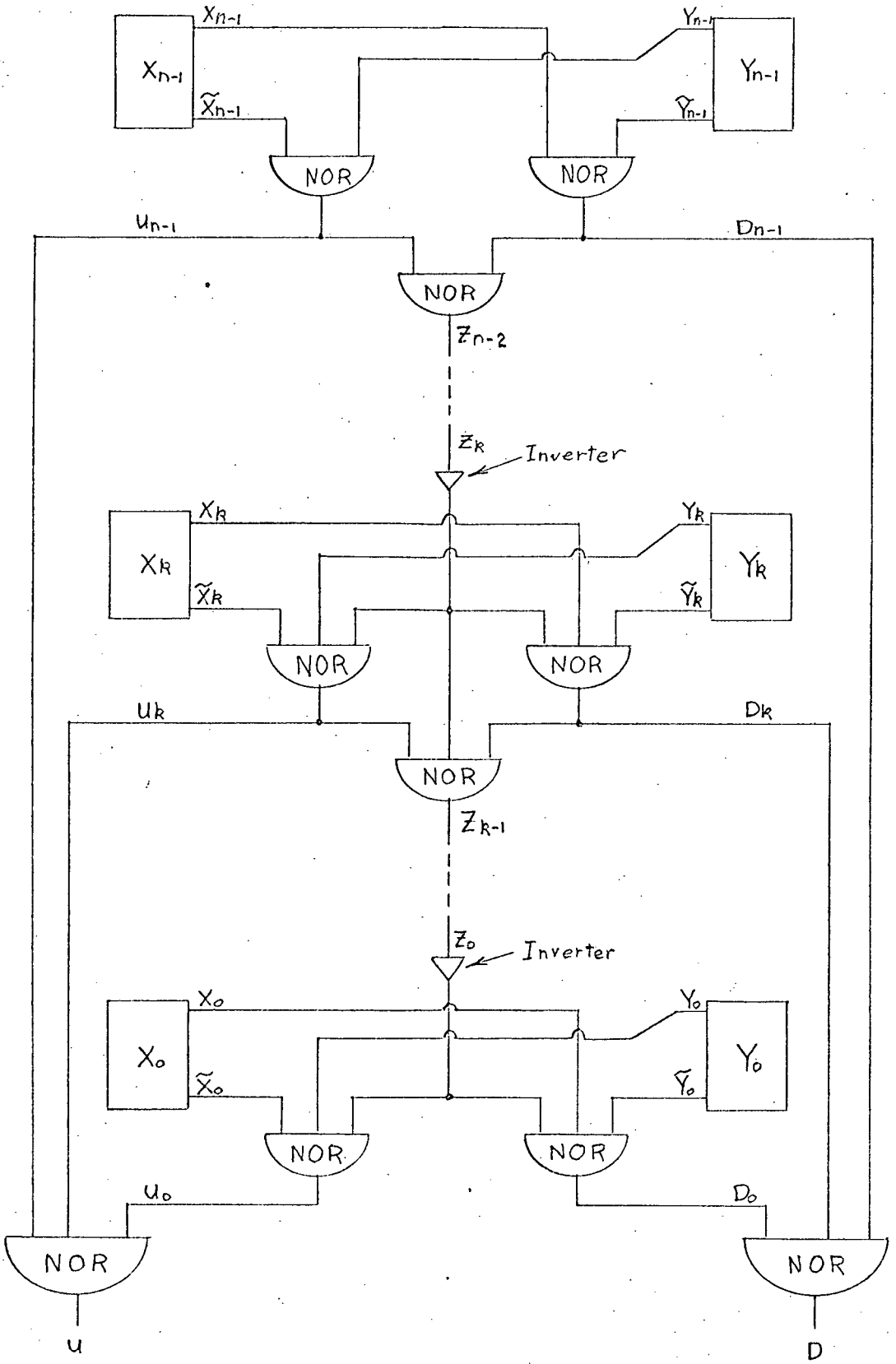

Fig. 4.4 Digital Comparator: $X = \sum_{R=0}^{n-1} 2^k X_k$. $Y = \sum_{k=0}^{n-1} 2^k Y_k$.

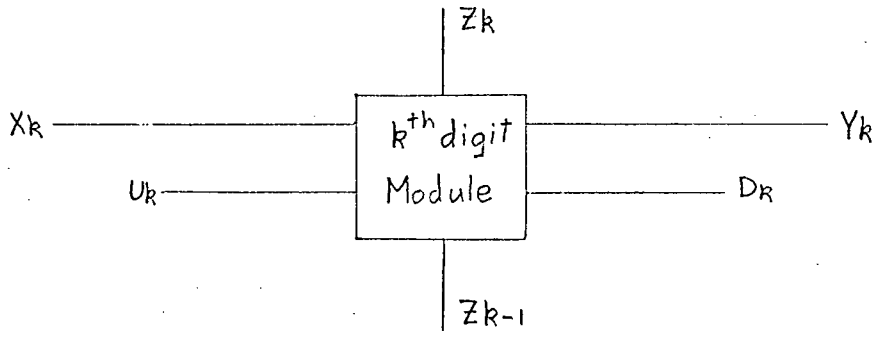

Z_k	X_k	Y_k	U_k	D_k	Z_{k-1}
0	0	0	0	0	0
0	0	1	0	0	0
0	1	0	0	0	0
0	1	1	0	0	0
1	0	0	0	0	1
1	0	1	0	1	0
1	1	0	1	0	0
1	1	1	0	0	1

Fig. 4.5 Truth table for the kth digit of the digital comparator

It follows that

$$U_k = \overline{Z_k + X_k + Y_k}$$

$$D_k = \overline{Z_k + X_k + Y_k}$$

$$Z_{k-1} = \overline{Z_k + U_k + D_k}$$

Fig. 4.4 is a realization of the truth table in Fig. 4.5.

4.4 The Up-Down Counter

Fig. 4.6 shows the schematic for three digits of an up-down counter. The counter was designed by Austin and is described in detail in his thesis.[22] It is basically a row of J-K flip-flops, each flip-flop being toggled by the same clock pulse. When U=0 and D=1, the counter counts up; when U=1 and D=0, the counter counts down. When U=D=1, the counter does not change. The state of each flip-flop is controlled by 3 NOR gates. In counting up, these gates do not permit a flip-flop to change to the ONE state unless all the lesser significant digits are in the ONE state. In counting down, the NOR gates prohibit a flip-flop from changing to the ZERO state unless all the lesser significant digits are in the ZERO state. When the counter is to remain unchanged, then the J-K rails are both made positive.

4.5 Binary Averager

A binary averager may be realized by shifting the output of a binary adder one digit towards the least significant bit. Fig. 4.7 shows the kth digit component of a binary adder which was built and tested. In Fig. 4.7, X_k and Y_k are the kth digits of $X = \sum_{k=0}^{n-1} 2^k X_k$ and $Y = \sum_{k=0}^{n-1} 2^k Y_k$, which are the two numbers being added, and S_k is the kth digit of the sum. Digit Z_k is the carry from the sum of the less significant digits. Fig. 4.8 shows the truth table for the kth digit.

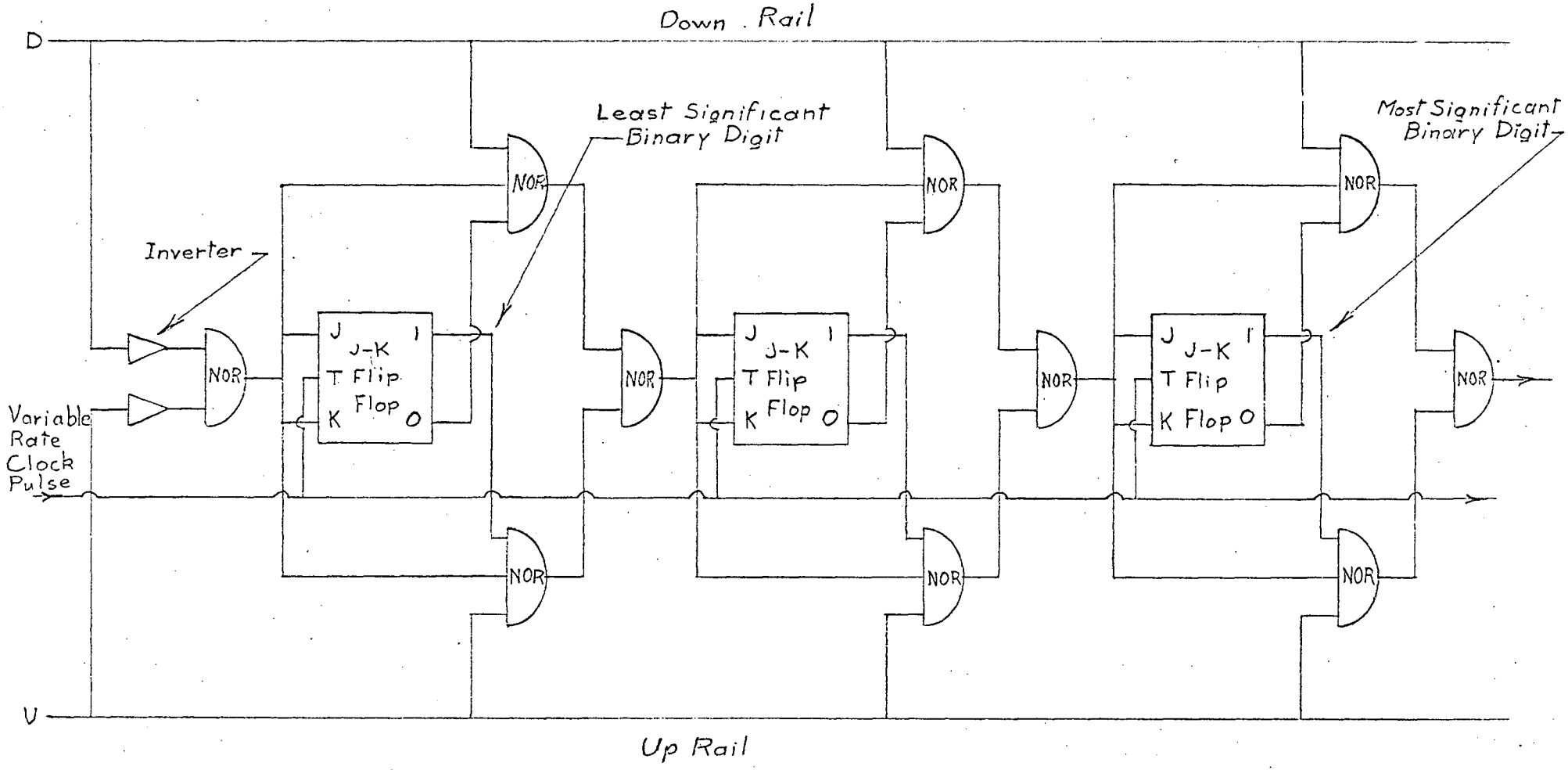

Fig. 4.6 3 Digit Portion of the Up-Down Counter

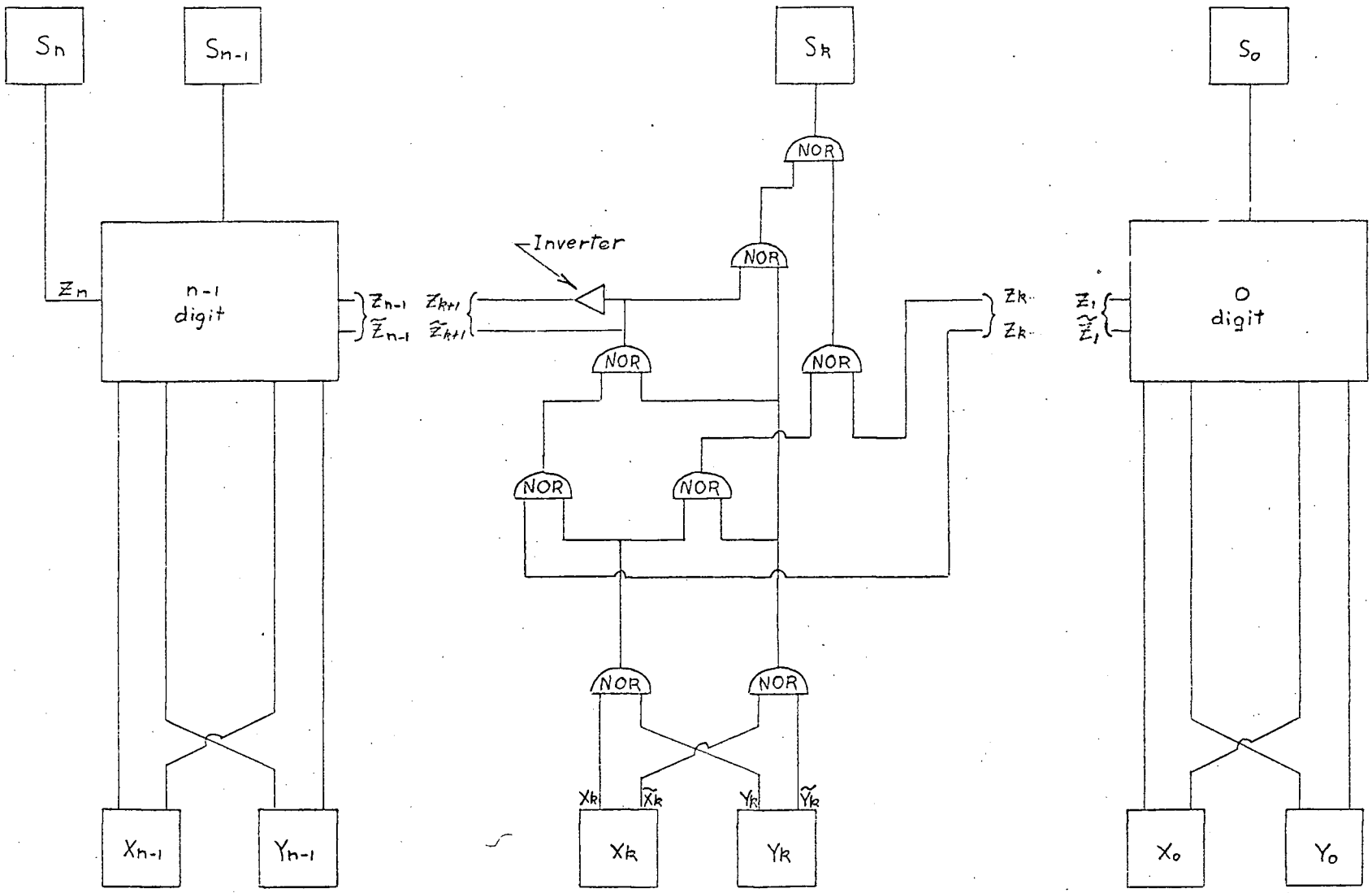

Fig. 4.7 Binary Adder. S = X + Y

X_k	Y_k	Z_k	S_k	Z_{k+1}
0	0	0	0	0
0	1	0	1	0
1	0	0	1	0
1	1	0	0	1
0	0	1	1	0
0	1	1	0	1
1	0	1	0	1
1	1	1	1	1

Fig. 4.8 Truth Table for k^{th} digit of a Binary Adder

Analysis of Fig. 4.7 show that

$$Z_{k+1} = X_kY_k + Y_kZ_k + Z_kY_k$$

and

$$S_k = (Z_k + \overline{X}_kY_k + X_k\overline{Y}_k)\overline{Z}_{k+1} + X_kY_kZ_k$$

Since digits Z_{k+1} and S_k have the same truth table as Fig. 4.8, the circuit in Fig. 4.7 is a binary adder.

4.6 Routing the Control Numbers to the Reactive Elements

The instantaneous value of each reactive element in the vocal tract analogue depends on the binary number in the J-K flip-flop memories of the digital comparator and the variable rate clock. In the final version of the analogue, these J-K flip-flops memories are to be arranged in matrix form as shown in

Fig. 4.9. The ith row corresponds to the ith reactive element. The jth column corresponds to the jth binary digit of the binary number that goes to the ith element. The J-K terminals in the jth column are common, and are connected through buffers to the output terminals of the jth flip-flop in the computer in-out register. The jth digit will be transferred from the computer to any toggled J-K flip-flop in the jth column. By toggling all J-K flip-flops in the ith row, the device selector transfers the binary number in the computer to the J-K memories of the digital comparator and the clock of the ith element.

The parameters of the analogue's excitation sources will be controlled in the same manner.

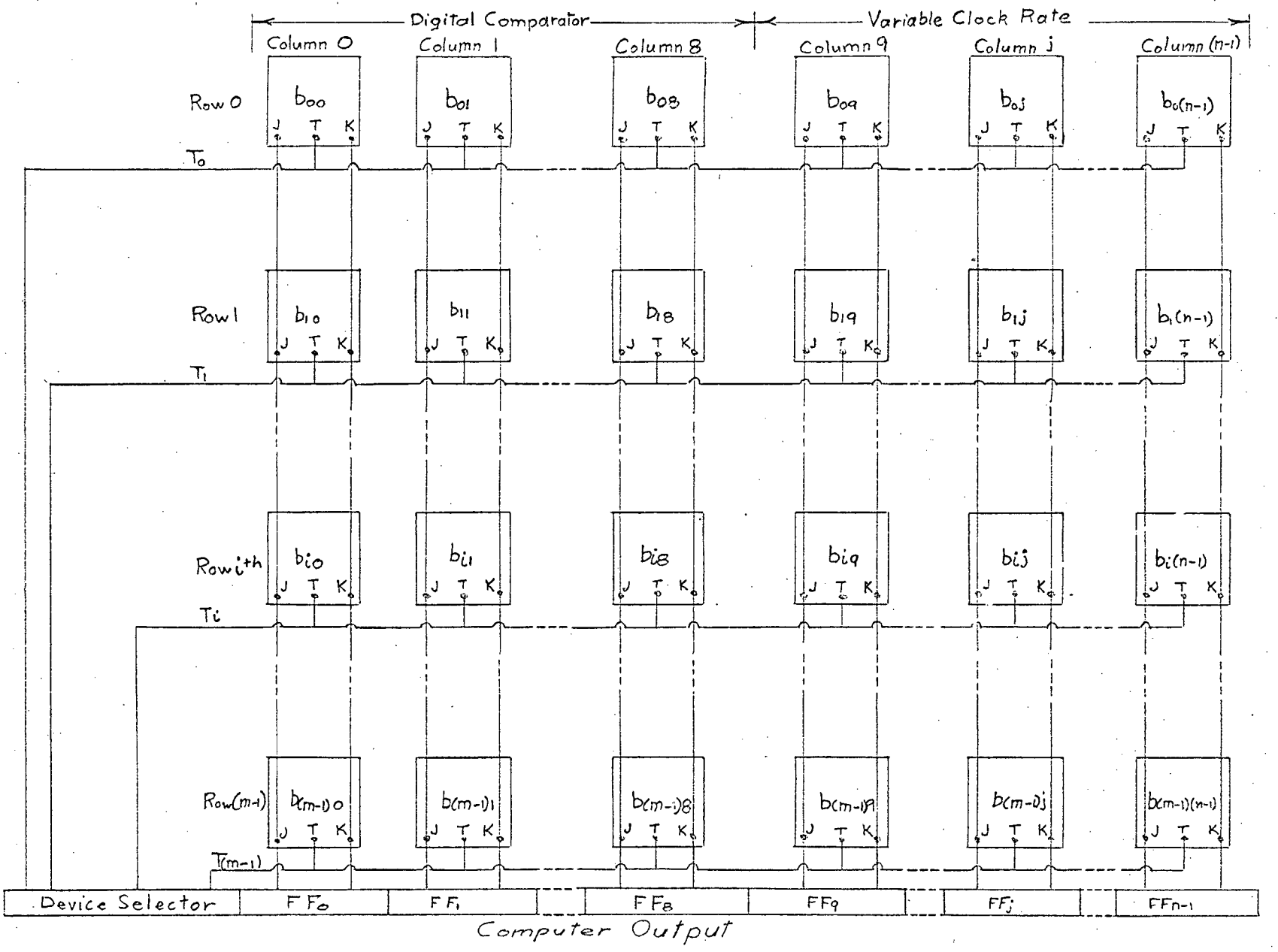

Fig. 4.9 Computer System for Routing Binary Numbers to Digital Comparators and Variable Rate Clocks. Each column corresponds to a separate binary digit:

5. THE TIME-VARYING INDUCTOR

5.1 Description of the Circuit

The variable inductor to be used in the analogue is based on the circuit in Fig. 3.3. Fig. 5.1 shows the circuit for $L = 10h/B$, where $B = \sum_{k=0}^{n-1} b_k 2^k$ and the b_k's are binary digits.

The inductance L is proportional to $R_1 = R/B$, where R is constant. Fig. 5.2 shows the control resistor R_1.

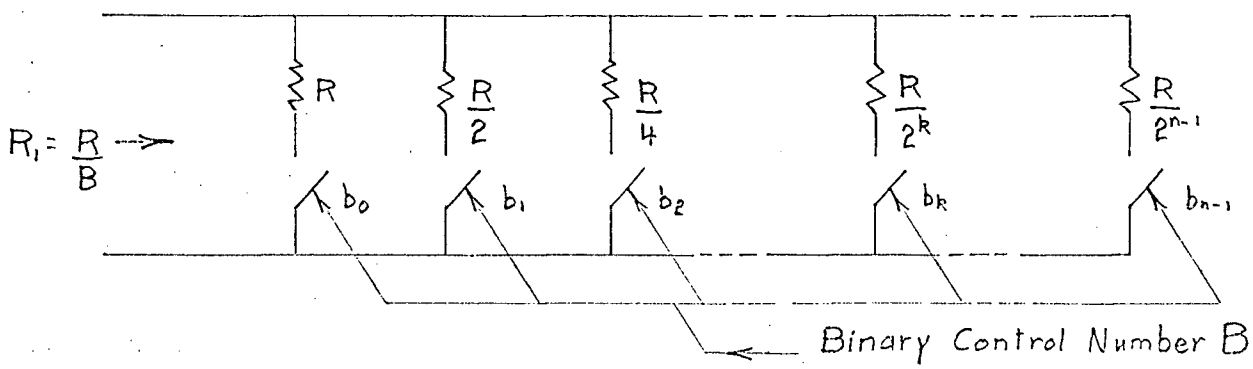

Fig. 5.2 Control Resistor R_1

If $b_k = 0$, the kth switch is open; if $b_k = 1$ the kth switch is closed. Thus,

$$\frac{1}{R_1} = \frac{1}{R} \sum_{k=0}^{n-1} 2^k b_k = \frac{B}{R} . \tag{5.1}$$

Fig. 5.3 shows the actual circuit for the kth resistor in

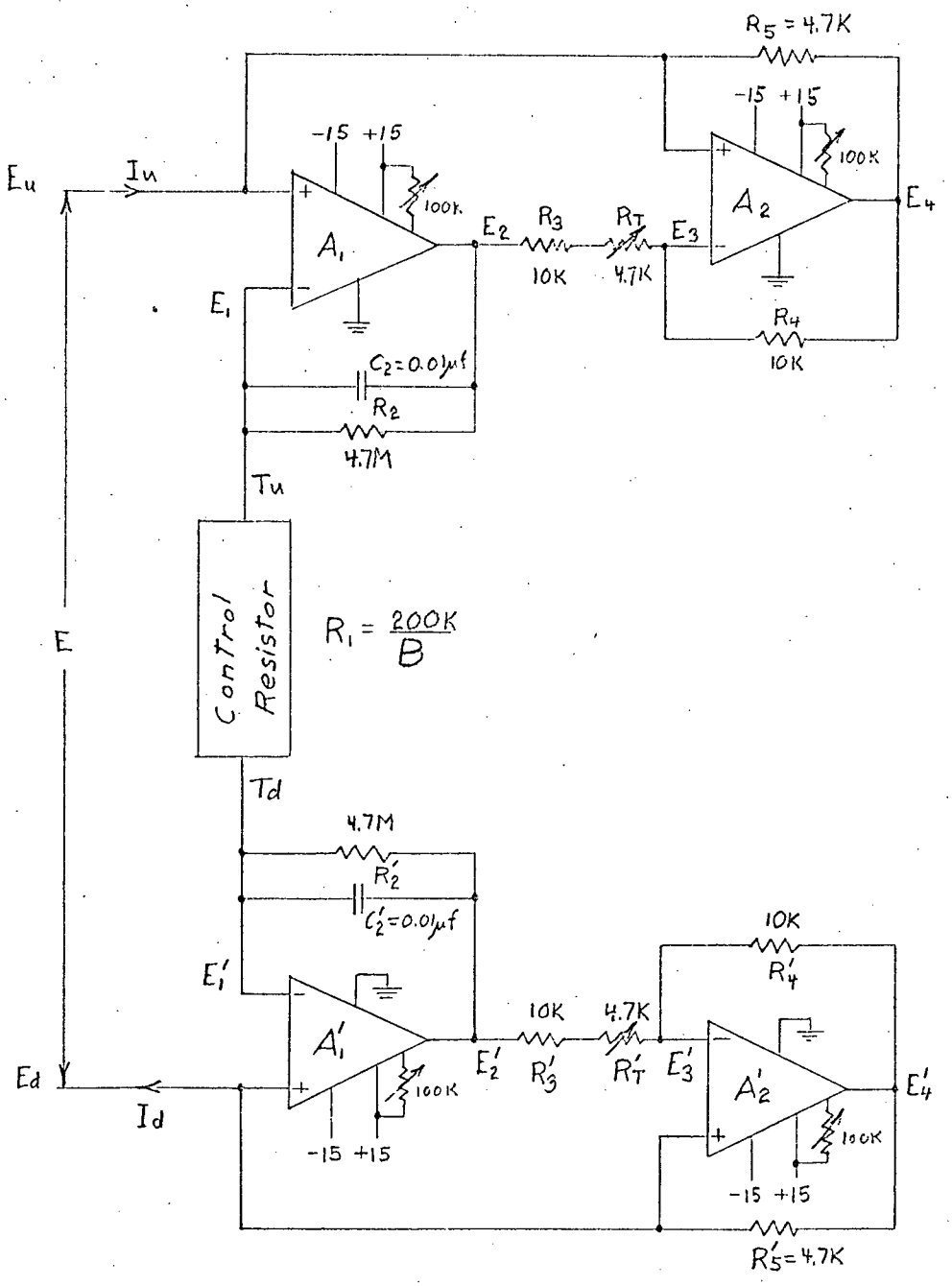

Fig. 5.1 Time-Varying Inductor

Fig. 5.2. The maximum voltage allowable at terminals T_u and T_d is $\pm$ 10 volts. Terminals T_u and T_d are connected to the inputs

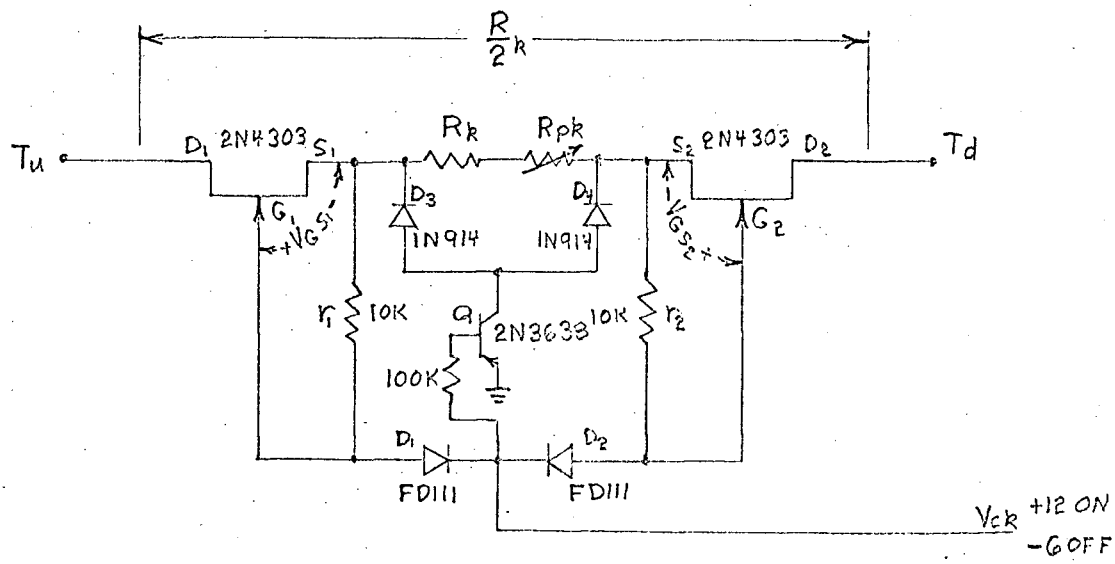

Fig. 5.3 Circuit for the kth Resistor in Fig. 5.2

of the different operational amplifiers in Fig. 5.1. Two FET's are needed for each switch to prevent the switching mechanism from contributing any input current to these amplifiers, which are sensitive to very small input currents.

When V_{ck} in Fig. 5.3 is equal to + 12 volts, transistor Q is OFF. Diodes D_1 and D_2 are back-biased, and there is no voltage drop across the resistors r_1 and r_2. Thus $V_{GS1} = V_{GS2} = 0$ and the FET's are ON. The only path that current can take is through the two FETs, variable pot R_{pk}, and resistor R'_k. By varying the value of pot R_{pk}, the total resistance $R_k = R'_k + R_{pk} + R_{ONk}$ (R_{ONk} is the total ON resistance of the two FET's) can be set accurately.

When $V_{ck} = -6$ volts the four diodes are forward biased and the transistor Q is ON. Gates G_1 and G_2 of the FETs are at -6 volts and sources S_1 and S_2 are approximately at ground. As a result, both FETs are OFF. Resistors r_1 and r_2 cannot be too large because they serve to discharge the capacitance of each FET.

The network in Fig. 5.4 was used to convert the binary digit b_k into the control voltage V_{ck} and at the same time turn on the lamp when $V_{ck} = +12$.

The outputs of amplifiers A_1 and A_1' in Fig. 5.1 depend only on the magnitudes of E_u, E_d and the circuit elements R_1, C_2 and C_2'

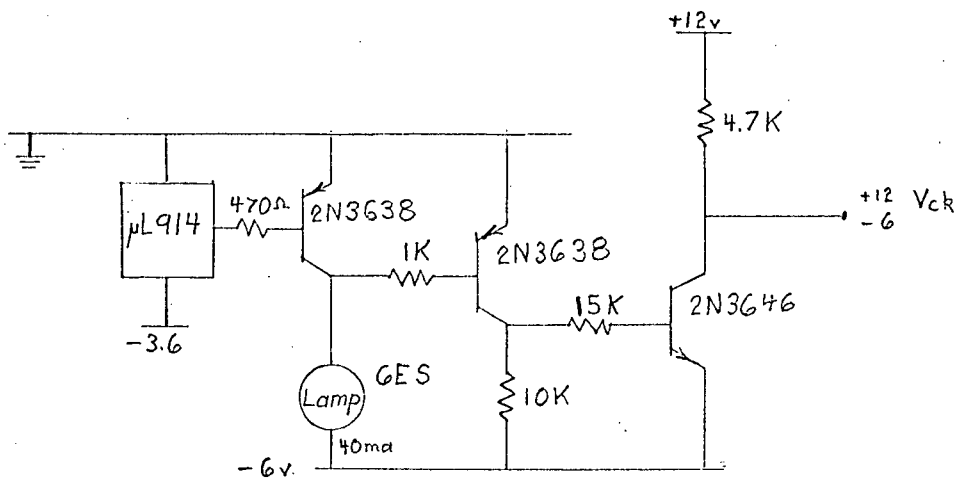

Fig. 5.4 Control Network for FET Switch

(Eqn. 3.4). Capacitors C_2 and C_2' are matched to prevent one input amplifier from saturating when the other does not. Large resistors R_2 and R_2' prevent the capacitors from charging up to the supply voltage when the input is grounded. The variable pots in series with R_3 and R_3' enable each inductor "half" to be set to an exact

inductance value. To prevent the amplifier outputs from saturating for large B, the input voltage E is limited to $\pm$ 2v. The input current is limited to $\pm 10v/R_5 \simeq \pm 2ma$; larger currents cause the amplifiers A_2 and A_2' to saturate. If R_5 is too small, the inductor circuit oscillates, since R_5 provides positive feedback path for amplifier A_2.

The inductor is calibrated by grounding points E_u and E_u' in Fig. 5.1 and adjusting the 100K trimming resistors on amplifiers A_1 and A_2 until first E_2 and then E_4 are zero. The impedance bridge is then connected to E_u and E_1', B is set to unity and R_T is adjusted to make the inductance equal to the required value. The procedure is repeated for the other half of the inductor.

5.2 Testing the Inductor

5.2.1 Steady State Inductor Tests

The inductor was tested in the time and frequency domain. The frequency domain tests yield measures of the inductor's quality factor Q and linearity with respect to control number B and frequency f. The time domain tests indicated how well the inductor would perform as the inductance changed with time.

Let L_p be the inductance for B=1. Inductance L_p is changed by changing capacitors C_2 and C_2' in Fig. 5.1 Fig. 5.5 shows L/L_p vs B for f = 1 KHz and L_p equal to 100h, 10h and 1.0h. The corresponding values of C_2 and C_2' are 0.1, 0.01 and 0.001 μμf, respectively.

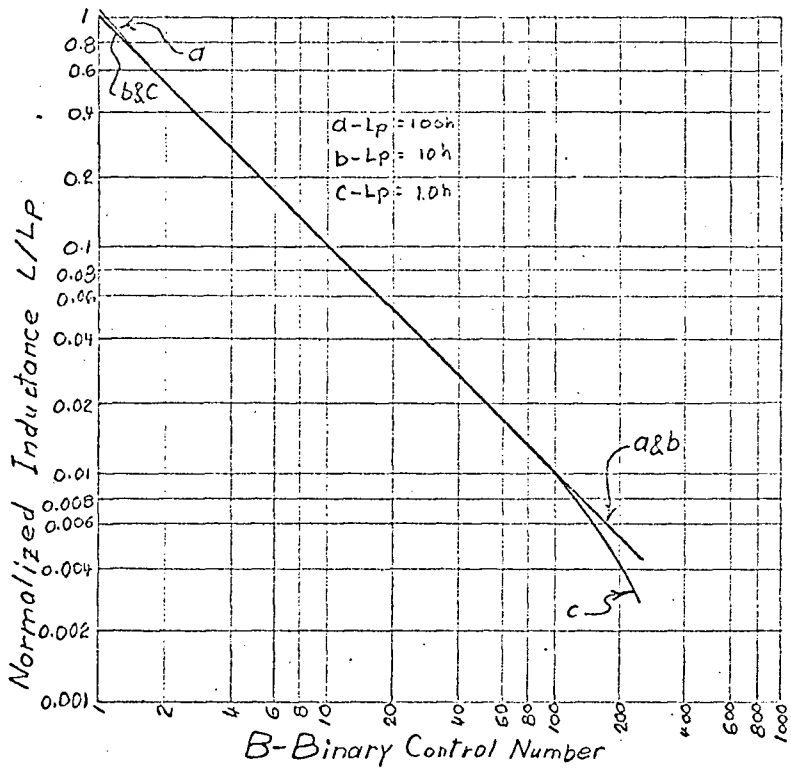

Fig. 5.5 Normalized Inductance L/L_p vs B for L_p = 100h, 10h and 1.0h, f = 1 KHz

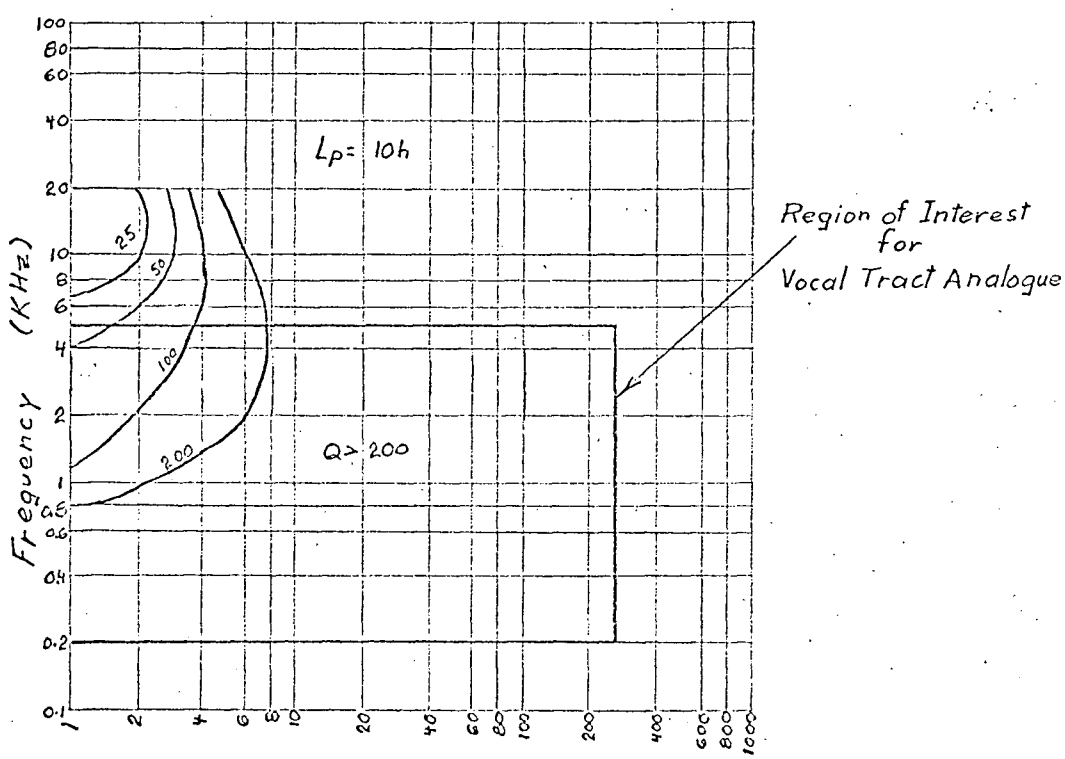

Fig. 5.6 Contours of Quality Factor Q. L_p = 10h

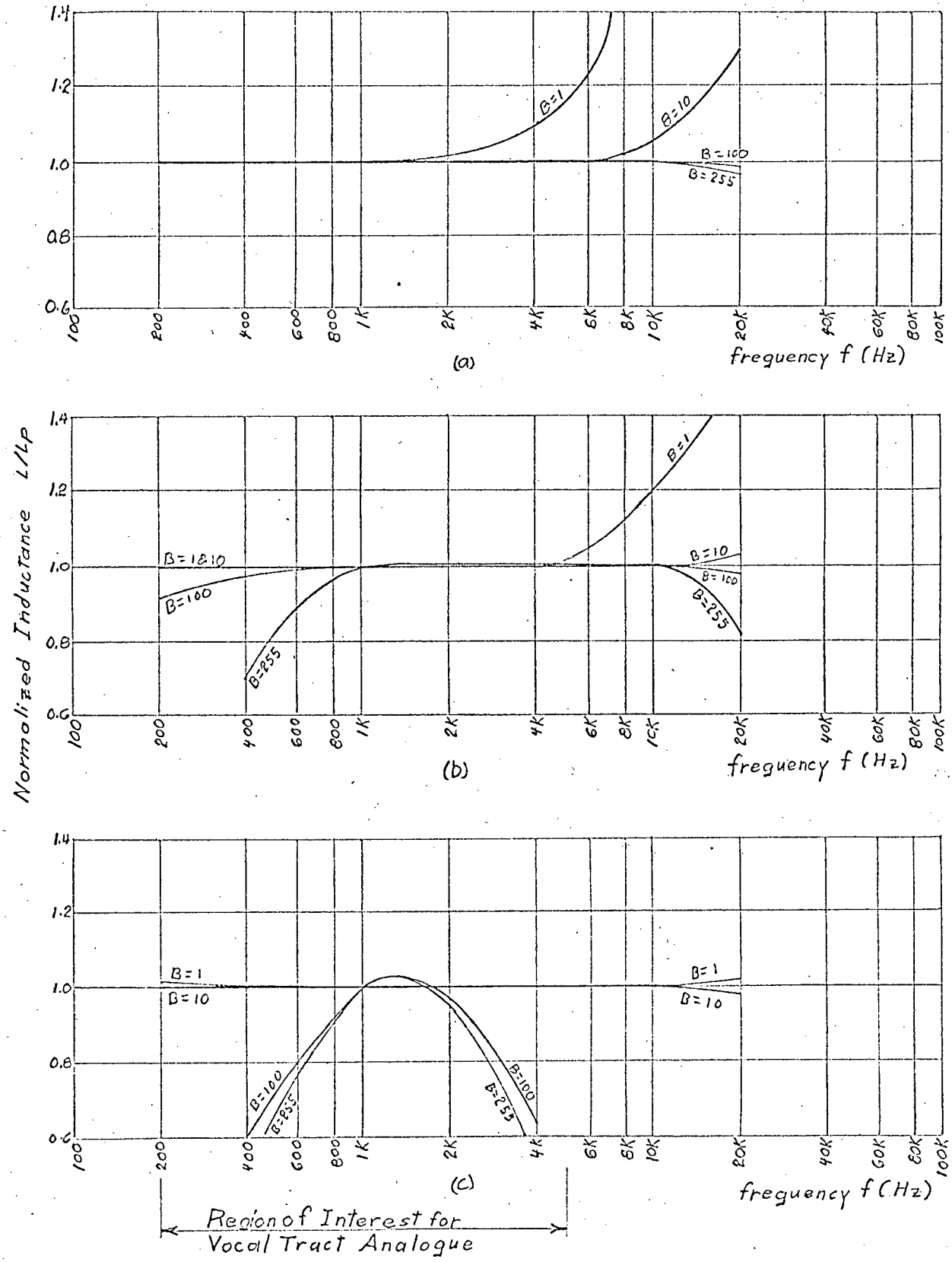

Fig. 5.7 Normalized Inductance L/L_p vs f, L_p and B, L_p is the inductance for B = 1 measured at f = 1 KHz
(a) L_p = 100h, (b) L_p = 10h and (c) L_p = 1.0h

Fig. 5.6 shows Q vs f and B. In the range required for use in the vocal tract analogue, the Q is far in excess of the required minimum of 50.

Fig. 5.7 shows normalized inductance vs f for B = 1, 10, 100 and 255 and for L_p = 100h, 10h and 1.0h. The range of operation needed for use in the vocal tract analogue is shown.

5.2.2 Transient Tests on the Time-Varying Inductor

The R-L circuit in Fig. 5.8 was used for the time-domain tests. With $e_i = EU_{-1}(t)$, the output $e_0(t)$ was measured on an

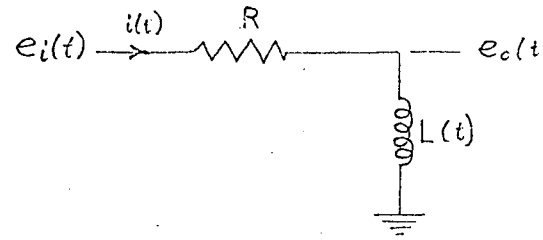

Fig. 5.8 Circuit for Inductor Time-domain Tests

oscilloscope and compared with the calculated output. The step function

$$U_{-1}(t) = \begin{cases} 0, & t < 0 \\ 1, & t > 0 \end{cases} .$$

The circuit was at rest for $t < 0$. Thus, $i(t) = e(t) = 0$ for $t < 0$. For $t > 0$, $e_0(t)$ can be calculated by taking the time derivative of the flux linkages $\lambda = Li$. Thus $e_0(t) = \frac{d\lambda}{dt}$, where

$$\frac{d\lambda}{dt} + \frac{R}{L(t)}\lambda = e_i \quad . \tag{5.1}$$

Eqn. 5.1 is of the form

$$\frac{dy}{dt} + P(t)y = Q(t) \quad . \tag{5.2}$$

The solution of eqn. 5.2 [23] is

$$y = e^{-\int P\,dt}\left[\int Q\, e^{\int P\,dt}\,dt\right] \tag{5.3}$$

The first time-domain test was made with $L(t) = L$, where L is a constant. For $e_i(t) = E\,U_{-1}(t)$,

$$e_0(t) = E\,e^{-\frac{Rt}{L}}\,U_{-1}(t) \; .$$

Fig. 5.9 shows a graph of the measured and calculated outputs $e_0(t)$ for $L = 10h$, $1h$, and $0.1h$, $E = 2$ volts and $R = 10K\Omega$. The calculated and measured values coincided almost exactly. Rounding at the top of the output at $t=0$ occurred for $L = 0.1h$. This rounding was caused by the finite slew rate of the operational amplifiers in Fig. 5.1. The output was measured using an oscilloscope with a variable time base. In the experiment L_p was equal to $10h$.

Consider $e_0(t)$ in Fig. 5.8 for $L(t) = L_p/B(t)$, where $B(t) = a \pm bt$, and a, b and L_p are positive constants. Equation 5.1 becomes

$$\frac{d\lambda}{dt} + \frac{R(a \pm bt)}{L_p}\lambda = E\,U_{-1}(t) \; . \tag{5.4}$$

From eqn. 5.2 it follows that for $t > 0$

R = 10K	
L	t/div
10h	0.5 msec/div
1h	50μsec/div
0.1h	5μsec/div

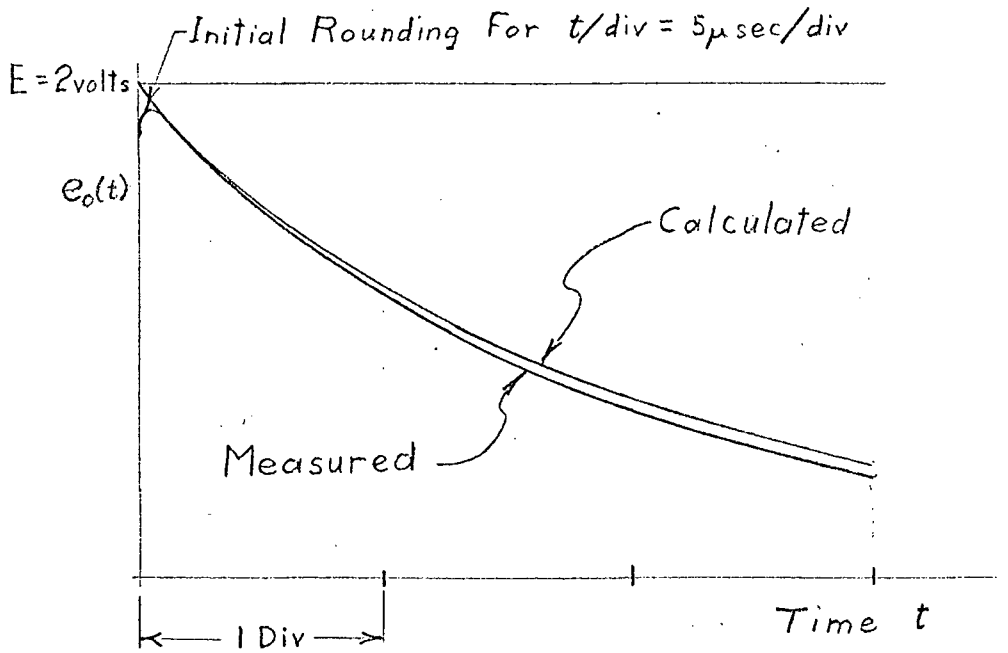

Fig. 5.9 Output $e_0(t)$ in Fig. 5.8 for L(t) Constant

$$\lambda(t)=E\, e^{-\frac{R}{L_p}(at \pm \frac{b}{2} t^2)} \int_0^t e^{\frac{R}{L_p}(ax \pm \frac{b}{2} x^2)} dx. \qquad (5.5)$$

The output voltage is the time derivative of equation 5.5

$$e_0(t) = E(1 - \frac{R}{L_p}(a \pm bt)e^{-\frac{R}{L_p}(at \pm \frac{b}{2} t^2)} \int_0^t e^{\frac{R}{L_p}(ax \pm \frac{b}{2} x^2)} dx). \qquad (5.6)$$

Now let B(t) be changed by unity at times $t=nT$ $(n=0,1,\ldots k\ldots N)$ where $T = \frac{1}{b}$. Thus,

$$B(t) = a \pm n \qquad nT \leq t \leq (n+1)T \qquad (5.7)$$

and

$$L(t) = \frac{L_p}{a \pm n} \qquad nT \leq t \leq (n+1)T. \qquad (5.8)$$

Eqn. 5.1 becomes for $nT \leq t \leq (n+1)T$

$$\frac{d\lambda}{dt} + \frac{R}{L_p}(a \pm n)\lambda = E\, U_{-1}(t). \qquad (5.9)$$

For $nT \leq t \leq (n+1)T$ the solution is

$$e_0(t) = E\left[1 - (a \pm n) \sum_{k=0}^{n-1} \frac{e^{-\frac{RT}{L_p}(n-k-1)(a\pm(\frac{n+k}{1}))}}{(a \pm k)}(1-e^{-\frac{RT}{L_p}(a\pm k)}) \right]$$

$$\times\, e^{-\frac{R}{L_p}(a\pm n)(t-nT)} \qquad (5.10)$$

The details of the solution are omitted, as they are similar to those to be presented in conjunction with eqn. 5.19.

In Fig. 5.1, $e_0(t) = L(t)\frac{di}{dt}$. In this case eqn. 5.1 becomes

$$L\frac{di}{dt} + Ri = E\,U_{-1}(t).$$

If $L(t) = L_p/B(t)$, where $B(t) = a \pm bt$ as defined for eqn. 5.4, then

$$\frac{di}{dt} + \frac{R(a \pm bt)}{L_p}\,i = \frac{E(a \pm bt)}{L_p}\,U_{-1}(t) \tag{5.11}$$

which is of the same form as eqn. 5.2. The solution of eqn. 5.11 for $t > 0$ is

$$i(t) = e^{-\frac{R}{L_p}(at \pm \frac{b}{2}t^2)} \int_0^t \frac{E(a \pm bx)}{L_p}\, e^{\frac{R}{L_p}(ax \pm \frac{b}{2}x^2)}\, dx. \tag{5.12}$$

Therefore $$e_0(t) = E\, e^{-\frac{R}{L_p}(at \pm \frac{b}{2}t^2)}. \tag{5.13}$$

When $L(t)$ is changed at times $t = nT$ and $B(t) = a \pm n$ as in eqn. 6.7, the solution of eqn. 5.2 is more difficult. Eqn. 5.1 becomes

$$\frac{di}{dt} + \frac{R}{L_p}(a \pm n)i = \frac{E(a+n)}{L_p}\,U_{-1}(t) \tag{5.14}$$

$$nT \le t \le (n+1)T.$$

Equation 5.14 is of the form of eqn. 5.2, with

$$P(x) = \frac{R}{L_p}(a \pm n) \qquad nT \le x \le (n+1)T.$$

The integrating factor in eqn. 5.2 becomes

$$e^{\int_0^t P(x)\,dx} = e^{\frac{R}{L_p}\left[(a\pm n)(t-nT) + (a\pm\frac{(n-1)}{2})nT\right]}$$

The solution of eqn. 5.14 for $nT < t < (n+1)T$ is

$$i(t) = e^{-\frac{R}{L_p}\left[(a\pm n)(t-nT) + (a\pm\frac{(n-1)}{2})nT\right]}$$

$$\times\left[\sum_{k=0}^{n-1}\int_{kT}^{(k+1)T}\frac{E(a\pm k)}{L_p}\,e^{\frac{R}{L_p}\left[(a\pm k)(x-kT)+(a\pm\frac{(k-1)}{2})kT\right]}dx\right.$$

$$\left.+\int_{nT}^{t}\frac{E(a\pm n)}{L_p}\,e^{\frac{R}{L_p}\left[(a\pm n)(x-nT)+(a\pm\frac{(n-1)}{2})nT\right]}dx\right] \qquad (5.15)$$

Integrating eqn. 5.15 gives

$$i(t) = e^{-\frac{R}{L_p}\left[(a\pm n)(t-nT) + (a\pm\frac{(n-1)}{2})nT\right]}$$

$$\times\left[\sum_{k=0}^{n-1}\frac{E(a\pm k)}{L_p}\left[\frac{L_p}{(a\pm k)R}\,e^{\frac{R}{L_p}\left[(a\pm k)(x-kT)+(a\pm\frac{(k-1)}{2})kT\right]}\right]_{x=kT}^{x=(k+1)T}\right.$$

$$\left.+\frac{E(a\pm n)}{L_p}\left[\frac{L_p}{(a\pm n)R}\,e^{\frac{R}{L_p}\left[(a\pm n)(x-nT)+(a\pm\frac{(n-1)}{2})nT\right]}\right]_{x=nT}^{x=t}\right. \qquad (5.16)$$

Rearranging eqn. 5.16 and substituting the limits gives

$$i(t) = \frac{E}{R}\, e^{-\frac{R}{L_p}\left[(a \pm n)(t-nT) + (a \pm \frac{(n-1)}{2})nT\right]}$$

$$\times \left[\sum_{k=0}^{n-1} e^{\frac{R}{L_p}(a \pm \frac{(k-1)}{2})kT} \left(e^{\frac{R}{L_p}(a \pm k)T} - 1\right) \right.$$

$$\left. + e^{\frac{R}{L_p}(a \pm \frac{(n-1)}{2})nT} \left(e^{\frac{R}{L_p}(a \pm n)(t-nT)} - 1\right) \right].$$

Rearranging gives

$$i(t) = \frac{E}{R} \left[1 - e^{-\frac{R}{L_p}(a \pm n)(t-nT)} \right.$$

$$\left. + \sum_{k=0}^{n-1} e^{-\frac{RT}{L_p}\left[(a \pm \frac{(n-1)}{2})n - (a \pm \frac{(k-1)}{2})k\right]} \left(e^{\frac{RT}{L_p}(a \pm k)} - 1\right) e^{-\frac{R}{L_p}(a \pm n)(t-nT)} \right].$$

The desired output $e_0(t) = e_i - Ri(t)$ is

$$e_o(t) = E\left[1 - \sum_{k=0}^{n-1} e^{-\frac{RT}{L_p}(n-k-1)(a \pm \frac{(n+k)}{2})} \left(1 - e^{-\frac{RT}{L_p}(a \pm k)}\right)\right] e^{-\frac{R}{L_p}(a \pm n)(t-nT)} \tag{5.17}$$

$$nT \leq t \leq (n+1)T .$$

To compare the measured output $e_0(t)$ of the circuit in Fig. 5.8 against the calculated output of eqns. 5.6, 5.10, 5.13, and 5.17, the number B(t) was varied as in Fig. 5.10 by the interpolating system described in Chapter 4. (See Fig.5.11). For the interval $0 \leq t \leq Tv = NT$ of Fig. 5.10, eqns. 5.6, 5.10, 5.13, and 5.17 were used to calculate the outputs. For the interval $t > Tv$, the outputs are as given by eqns. 5.10 and 5.17 with n=N. For eqns. 5.6 and 5.13, the outputs are decaying exponential of the form $e = E_c\, e^{-\frac{t}{\tau}}$ where $\tau = L_p/R(a \pm bTv)$ and E_c is the value of $e_0(t)$ in eqns. 5.6 or 5.13 at t=Tv. The outputs were calculated and plotted by an IBM 7040 computer for $b = 4/3 \times 10^5$/sec, N = 40, Tv = 0.3 msec and for a=4 and a=44. (See Figs.5.12 and 5.13). The discrepancy between $e_0(t)$ for the continuous L(t) and the corresponding stepwise approximation was so small that only $e_0(t)$ calculated from eqns. 5.10 and 5.13 are shown. The calculated results in Fig. 5.12 for the true inductor do not agree very well with the calculated and measured results in Fig. 5.13. The discrepancy is noticable because the rate of change of inductance is of the same order of magnitude as the rate of change of current i(t). Fortunately, this problem will not occur in the vocal tract analogue. The close agreement between the calculated and measured values for the device for which $e(t) = L(t)\,\frac{di}{dt}$ indicates its accuracy and the effectiveness of the interpolating system.

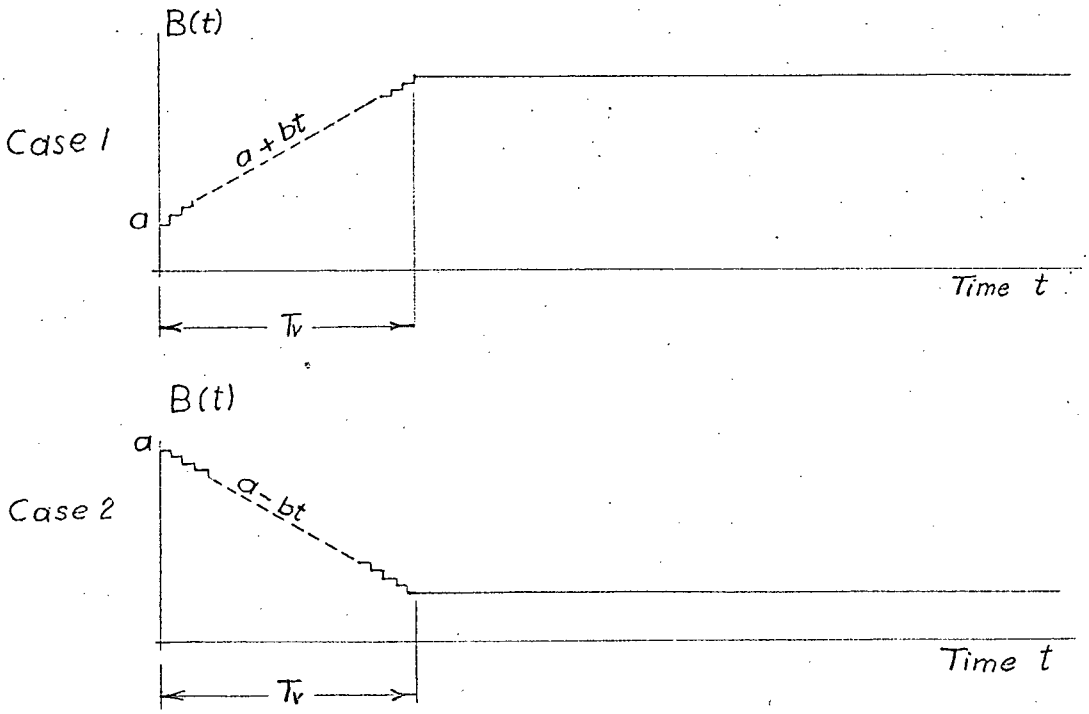

Fig. 5.10 Variation of Binary Number B controlling the Time-Varying Inductor

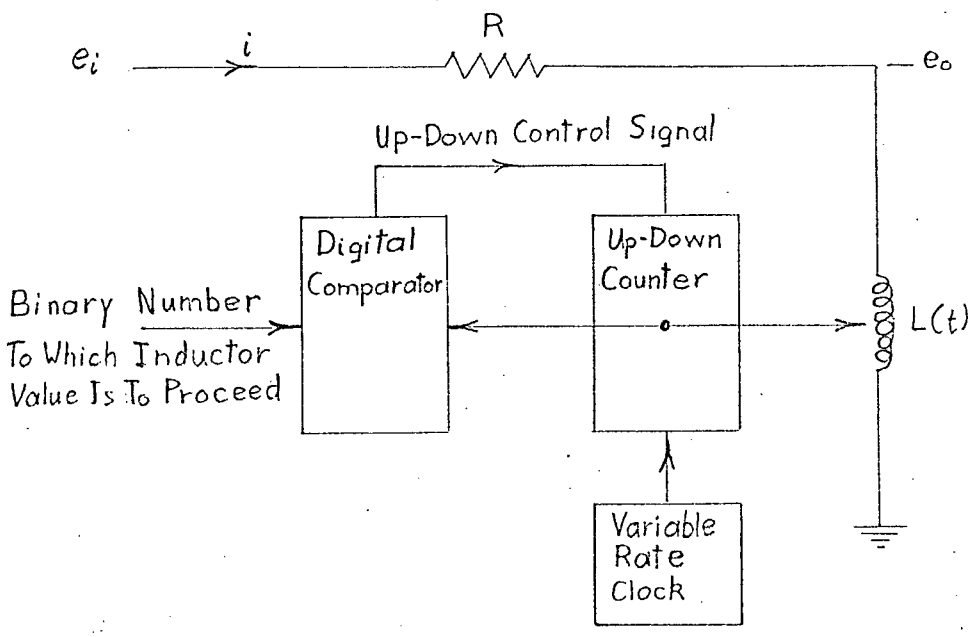

Fig. 5.11 Time-Varying Inductor Test Arrangement

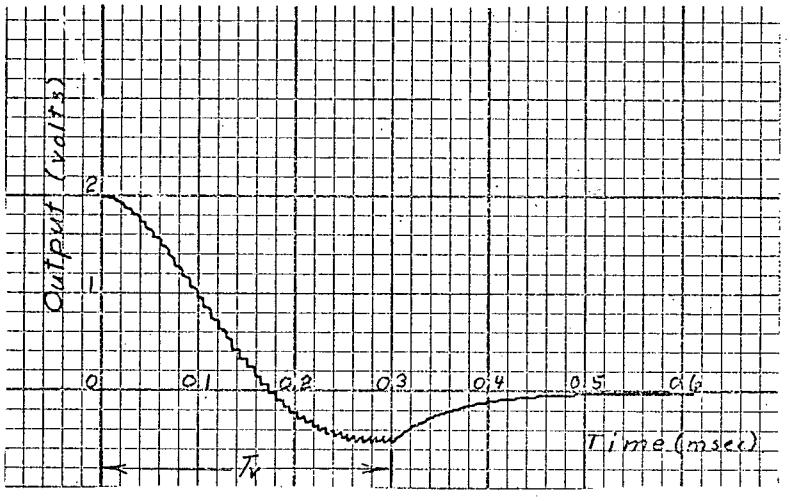

(a)

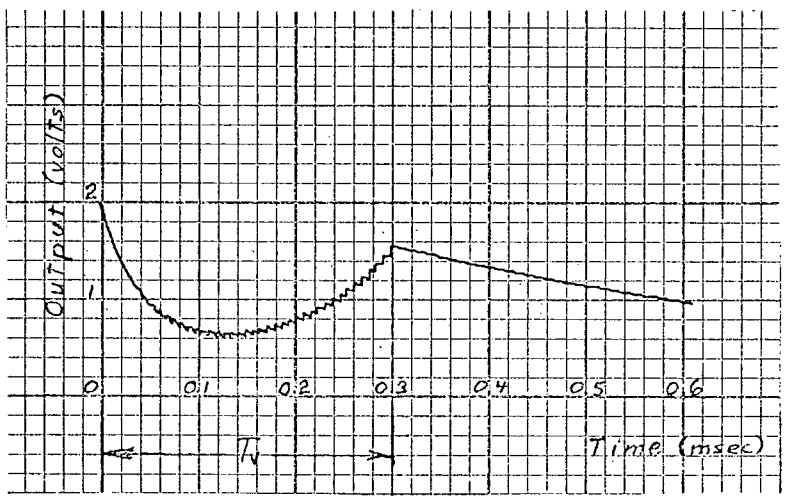

(b)

Fig. 5.12 Calculated Outputs for R-L Circuits in Fig. 5.8 for the True Time-varying Inductance $e_0(t) = \frac{d(Li)}{dt}$, where $L = 10h/(a \pm bt)$ for $0 \leq t \leq T_v$ and $b = \frac{4}{3} \times 10^5$/sec (a) $L = 10h/(a+bt)$; $a = 4$. (b) $L = 10h/(a-bt)$; $a = 44$.

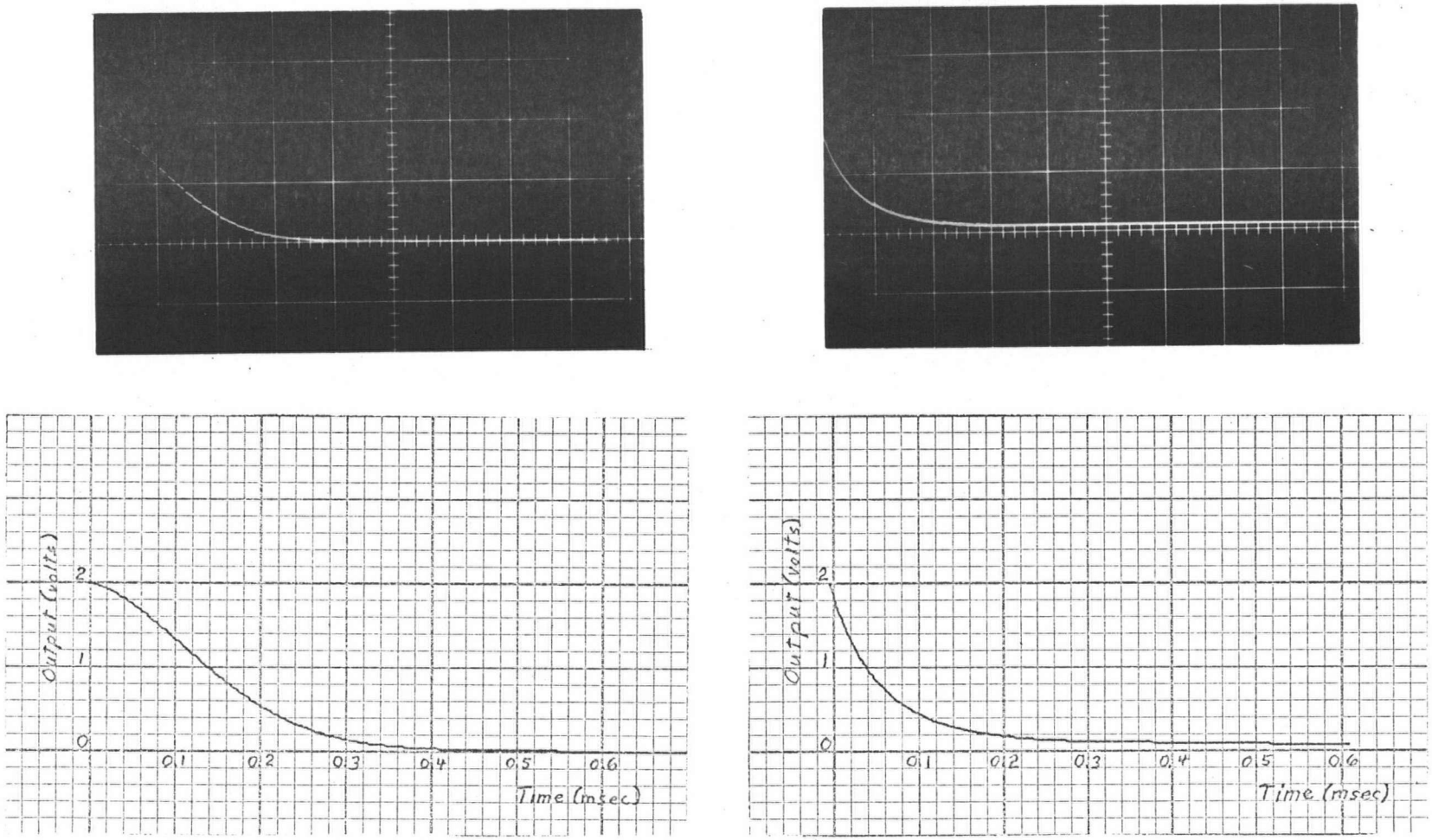

(a) (b)

Fig. 5.13 Calculated and Measured Output for R-L Circuit in Fig. 5.8, $e_0(t) = L(t)\frac{di}{dt}$. Upper Photographs: Vertical Scale; 1 volt/div, Horizontal Scale; 0.1 msec/div. Lower Graphs: Calculated Outputs.
(a) $L = 10h/(a+bt)$ where $a=4$ and $b = 4/3 \times 10^5$/sec.
(b) $L = 10h/(a-bt)$ where $a=44$ and $b= 4/3 \times 10^5$/sec.

6. THE TIME-VARYING CAPACITOR

6.1 Description of the Circuit

The time-varying capacitor in Fig. 6.1 is based on the circuit in Fig. 3.2. Fig. 6.1 shows the circuit for $C = (0.0037)\,B\ \mu f$. The capacitance is varied in the same manner as the inductance, namely, by varying the control resistor $R_1 = R/B$, where R is constant and $B = \sum_{k=0}^{n-1} 2^k\, b_k$. The same general technique used for varying the resistor R_1 in Fig. 5.2 is used here. The actual circuit is simpler, however, since the capacitor in the vocal tract analogue is grounded. Fig. 6.2 shows the variable resistor R_1.

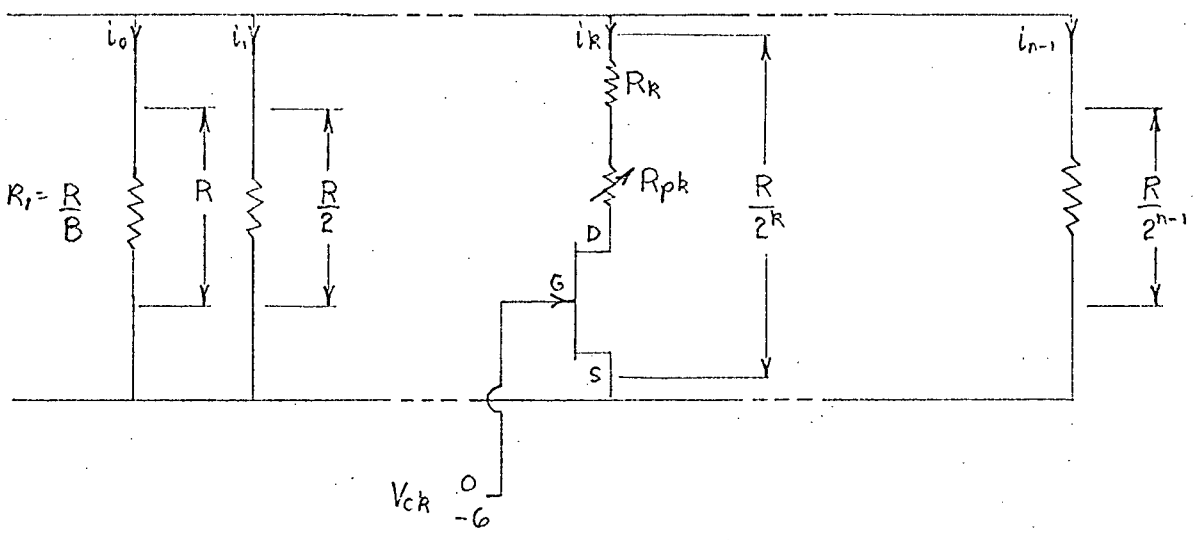

Fig. 6.2 Control Resistor R_1 for the Time-Varying Capacitor

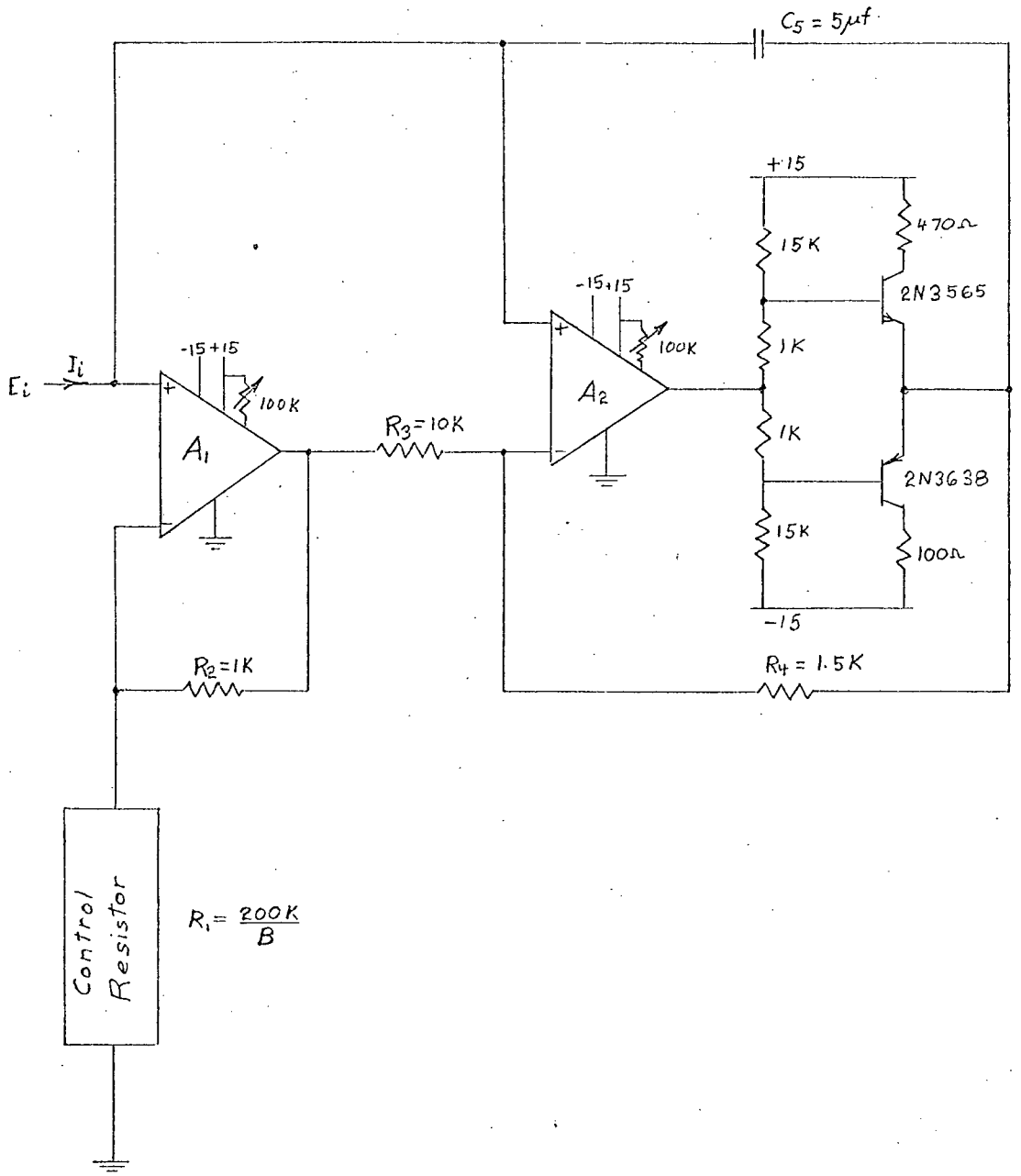

Fig. 6.1 Time-Varying Capacitor

When $V_{ck} = 0$, the kth FET is ON. When $V_{ck} = -6$ volts, the kth FET is OFF and $i_k = 0$. FETs rather than transistors are used for switches since $-10v \leq V_{DS} \leq 10v$. The resistance $R_k + R_{pk} + R_{ONk}$ is adjusted by the variable resistor R_{pk}, where R_{ONk} is the ON resistance of the kth FET.

The circuit in Fig. 6.3 converts the binary digit b_k into the control voltage V_{ck} and at the same time turns on the lamp when the kth FET is ON.

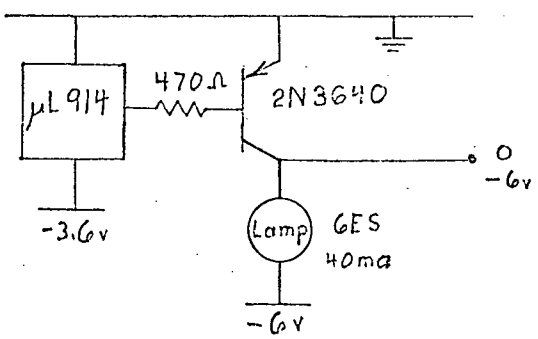

Fig. 6.3 FET Switch Driver

The booster circuit which terminates the operational amplifier in Fig. 6.1 is a totem pole emitter follower capable of delivering ± 20 ma. Its purpose is to provide more output current than the inadequate amount supplied by the operational amplifier. The input voltage E_i to the variable capacitor is limited to approximately ± 4 volts. A higher input voltage will saturate

amplifier A_1, when B is large. The input current is limited to the maximum output of the booster, $\pm$ 20 ma.

6.2 Testing the Capacitor

6.2.1 Steady State Capacitor Tests

The time and frequency domain tests for the capacitor were similar to those for the inductor.

Let C_p be the capacitance for B=1, f = 1 KHz. Capacitance C_p is changed by changing capacitor C_5 in Fig. 6.1 Fig. 6.4 shows C/C_p vs B for C_p = 3750 μμf, 375 μμf and 75 μμf. The corresponding values of C_5 are 5μf, 0.5μf and 0.1μf.

Fig. 6.5 shows Q as a function of frequency and B. In the range required for use in the vocal tract analogue, the Q is much in excess of the required minimum of 50.

Fig. 6.6 shows C/C_p vs frequency for B=1, 10, 100 and 255 and for C_p = 3750 μμf, 375 μμf and 75 μμf. The range of operation needed for use in the vocal tract analogue is shown. For each set of curves, the non-linear behaviour of C/C_p vs f for B=1 is due mainly to stray capacitance in parallel with the control resistor. This stray capacitance will be reduced, when the control resistor is mounted on a printed circuit board.

6.2.2 Transient Tests on the Time-varying Capacitor

To make time domain tests of the capacitor the R-C circuit in Fig. 6.7 was used. With $e_i(t) = E\,U_{-1}(t)$, the output $e_0(t)$ was

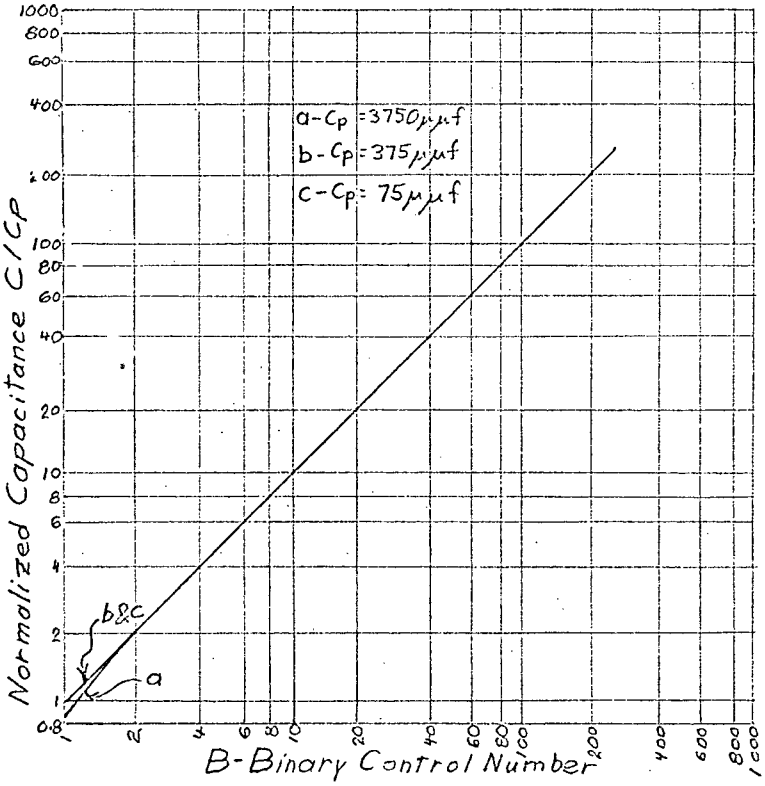

Fig. 6.4 Normalized Capacitance C/C_p vs B for C_p = 3750 μμf, 375 μμf and 75 μμf. f = 1 KHz

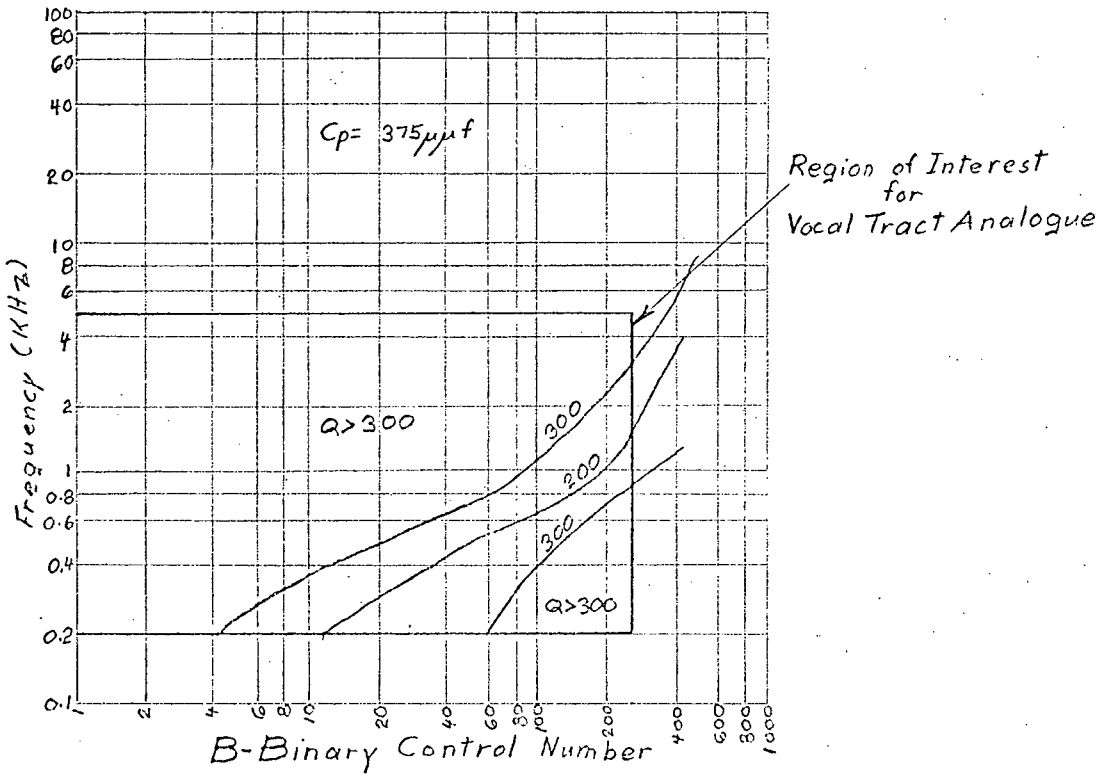

Fig. 6.5 Contours of Capacitor Quality Factor Q

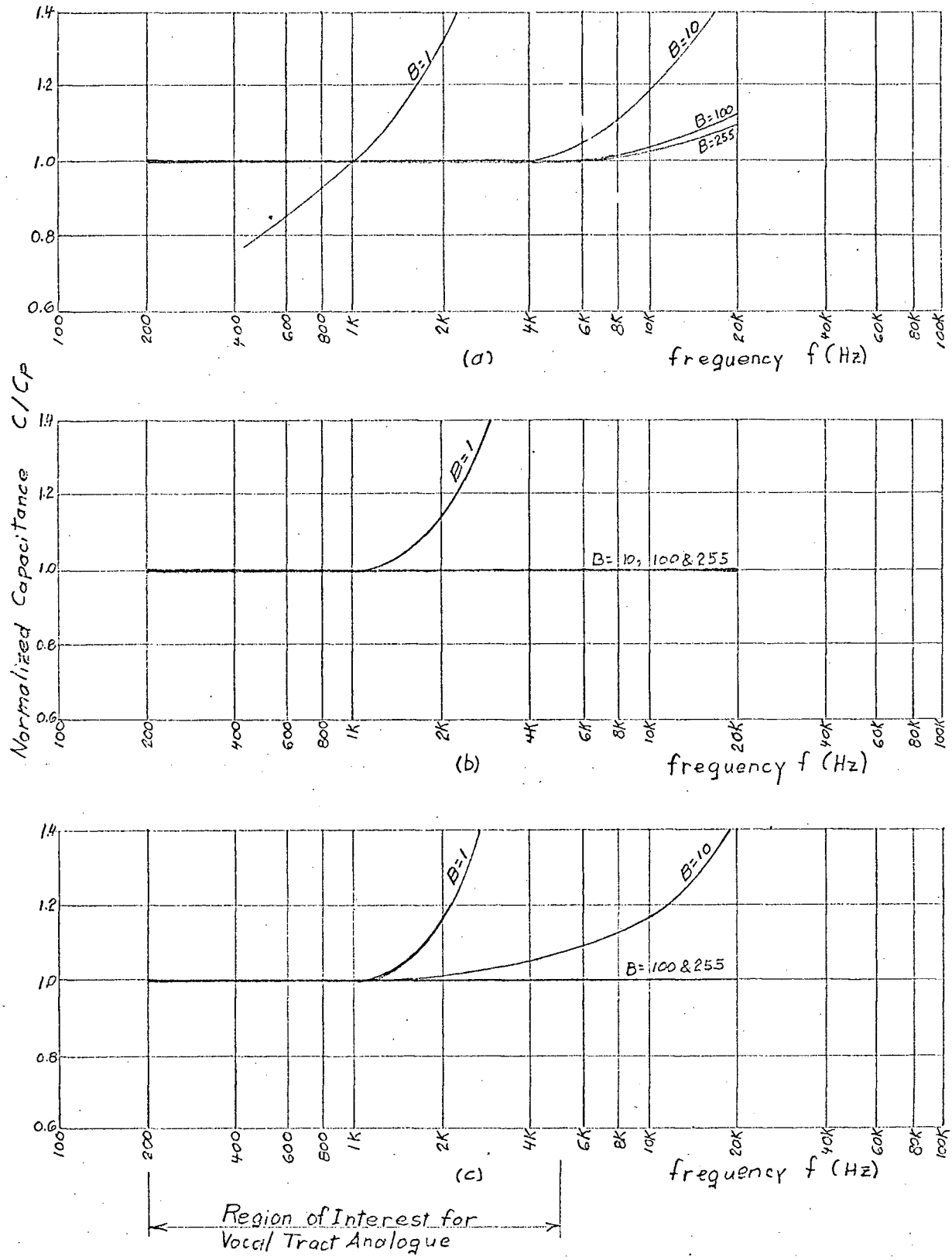

Fig. 6.6 Capacitance C/C_p vs f, C_p and B. C_p is the capacitance for B = 1 measured at f = 1 KHz

measured on an oscilloscope and compared with the calculated output.

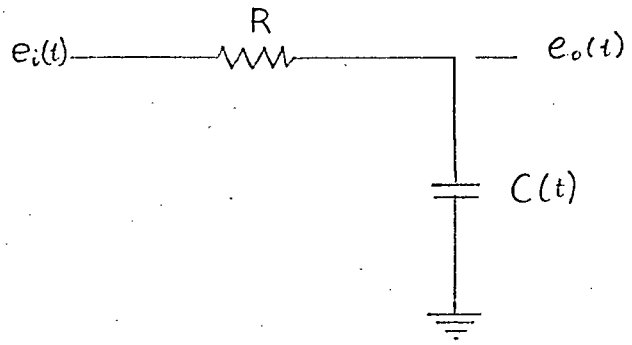

Fig. 6.7 Circuit for Capacitor Time Domain Tests

The circuit was at rest for $t < 0$. Thus, $i(t) = e(t) = 0$ for $t < 0$. For $t > 0$, $e_0(t)$ is best calculated by finding the charge $q(t)$ stored on the capacitor and then dividing by the capacitance.

Thus $e_0(t) = q(t)/C(t)$, and

$$\frac{dq}{dt} + \frac{q}{RC(t)} = \frac{e_i}{R} \tag{6.1}$$

Eqn. 6.1 is cf the form of eqn. 5.2.

The first time-domain test was made with $C(t) = C$, where C is a constant. For a step input

$$e_0(t) = E(1 - e^{-\frac{t}{RC}})U_{-1}(t)$$

Fig. 6.8 shows the measured and calculated outputs $e_0(t)$ for

C = 0.006 μf, 0.06 μf, 0.3 μf and E = 2 volts. The lowest value of capacitance was not used because Fig. 6.6 shows that for B = 1 the capacitance is a highly non-linear function of frequency. This nonlinearity causes a large ringing effect in the output.

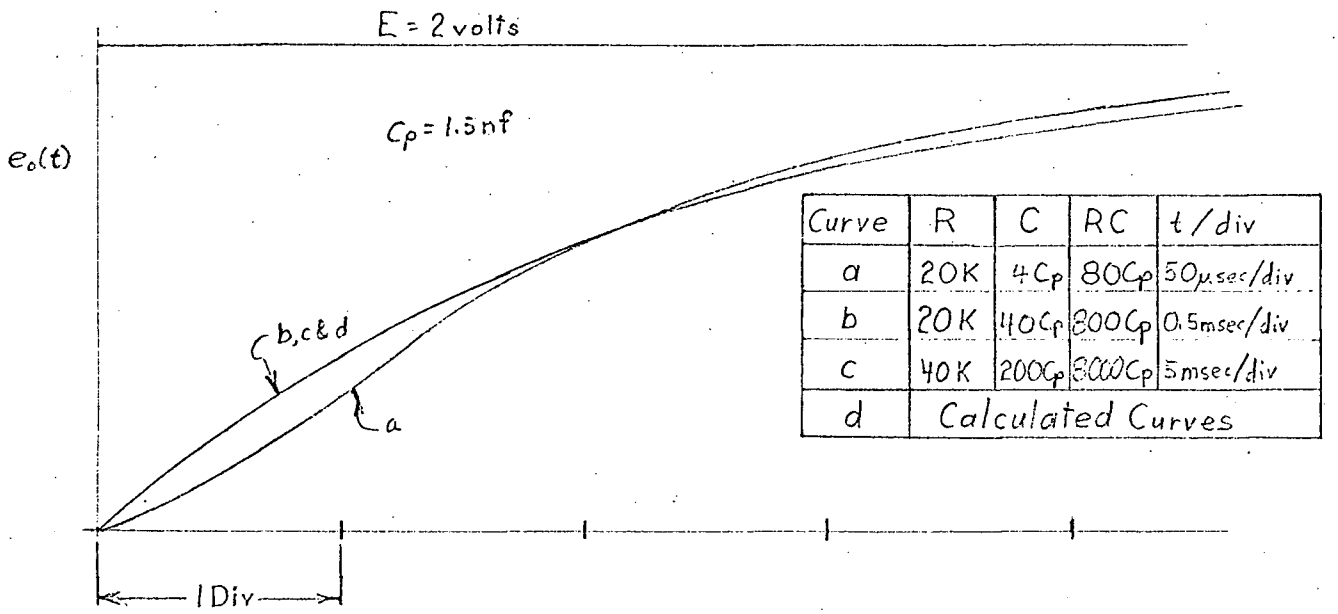

Fig. 6.8 Output $e_0(t)$ for Constant Capacitance

The output was measured using an oscilloscope with a variable time base. In the experiment C_p was equal to 1.5 nf.

When $C(t) = C_p\ B(t)$ was time-varying, B(t) and $e_i(t)$ were as shown in Fig. 6.9. The number B(t) was varied by using the interpolating system for the vocal tract analogue, as shown in Fig. 6.10.

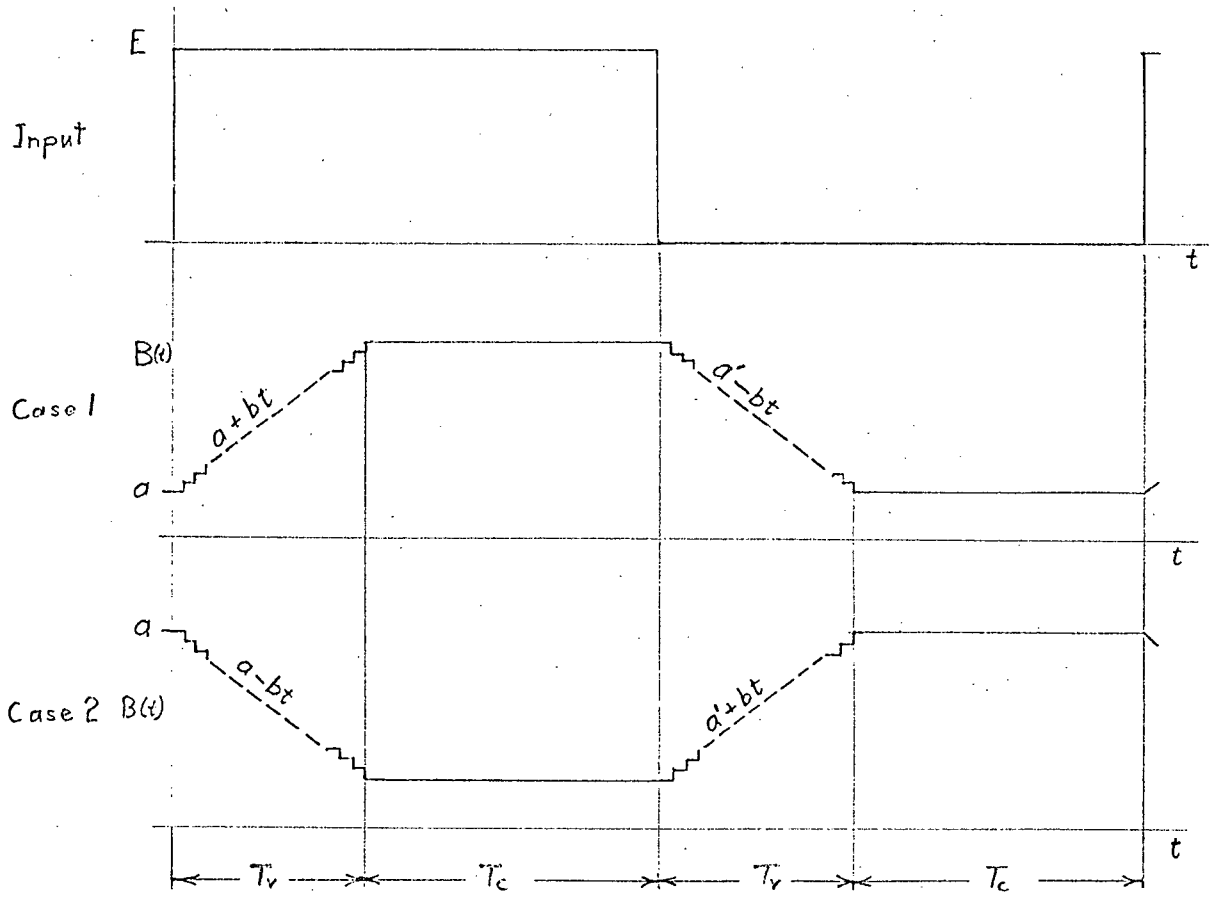

Fig. 6.9 Inputs to R-C Network in Fig. 6.10

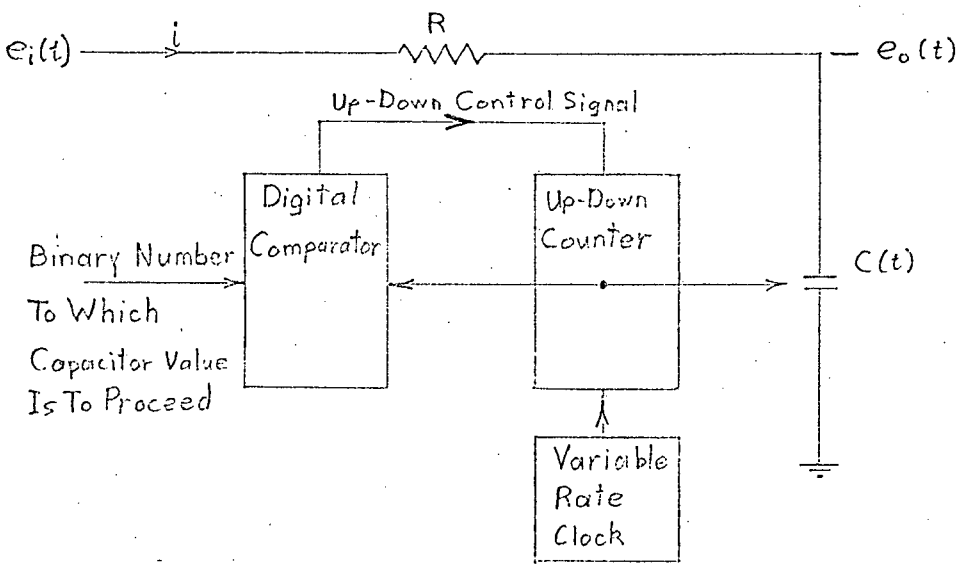

Fig. 6.10 Time-Varying Capacitor Test Arrangement

If $e_i(t)$ is as shown in Fig. 6.9, and if $C(t) = C_p B(t)$ and $B(t) = a \pm bt$ where C_p, a, and b are positive, then eqn. 6.1 becomes for $0 < t < Tv$

$$\frac{dq}{dt} + \frac{q}{RC_p(a \pm bt)} = \frac{E}{R} \; U_{-1}(t) \tag{6.2}$$

The exponent $\int P \, dt$ of the integrating factor becomes

$$\int P \; dt = \int \frac{dt}{RC_p(a \pm bt)} = \frac{\ln |a \pm bt|}{\pm b \, RC_p}$$

The solution of eqn. 6.2 is

$$q(t) = e^{-\frac{\ln(a \pm bt)}{\pm bRC_p}} \int_0^t \frac{E}{R} \, e^{\frac{\ln(a \pm bx)}{\pm bRC_p}} \, dx$$

$$= \frac{C_p E}{(1 \pm bRC_p)} \left[(a \pm bt) - a\left(\frac{a}{a \pm bt}\right)^{\pm \frac{1}{bRC_p}} \right] \qquad bRC_p \neq 1 \quad a \pm bt > 0$$

Since $e_0(t) = q(t)/C(t)$,

$$e_0(t) = \frac{E}{(1 \pm bRC_p)} \left[1 - \left(\frac{a}{a \pm bt}\right)^{\frac{bRC_p \pm 1}{bRC_p}} \right] \qquad bRC_p \neq 1 \quad a \pm bt > 0 \tag{6.3}$$

For $Tv \leq t \leq Tv + Tc$, capacitance $C_p(a \pm b \, Tv)$ remains constant, and the output goes exponentially to a value of E_0 at the end of the first half of the square wave.

$$E_0 = E - (E - E') \, e^{-\frac{Tc}{RC_p(a \pm bTv)}} \tag{6.4}$$

where $E' = \frac{E}{(1 \pm bRC_p)} \left[1 - \left(\frac{a}{a \pm bT_v}\right)^{\frac{bRC_p \pm 1}{bRC_p}} \right]$

$$\simeq \frac{E}{(1 \pm bRC_p)} \qquad \text{if} \qquad \left(\frac{a}{a \pm bTv}\right)^{\frac{bRC_p \pm 1}{bRC_p}} << 1$$

During the second half cycle of the square wave,

$$\frac{dq}{dt} + \frac{q}{RC_p(a' \pm bt)} = 0, \tag{6.5}$$

where time t is measured from the start of the negative going step in the square wave. The initial charge on the capacitor at $t = 0$ is $Q_0 = a'C_p E_0$. Let $B(t) = a' \pm bt$, where a' and b are positive. Rearranging eqn. 6.5 and integrating gives

$$q(t) = a'C_p E_0 \left(\frac{a'}{a' \pm bt}\right)^{\pm \frac{1}{bRC_p}} \qquad 0 \leq t \leq Tv$$

Since $e_0(t) = q(t)/C(t)$,

$$e_0(t) = E_0 \left(\frac{a'}{a' \pm bt}\right)^{\frac{bRC_p \pm 1}{bRC_p}} \qquad 0 \leq t \leq Tv \tag{6.6}$$

During the time $Tv \leq t \leq Tv + Tc$, (t is again measured from the start of the negative going step in the square wave), the capacitance remains constant at $C = C_p(a' \pm b\,Tv)$ and $e_0(t)$

decays exponentially to zero.

$$e_0(t) = E_0' \; e^{-\frac{(t - Tv)}{RC_p(a' \pm bTv)}} \tag{6.7}$$

where

$$E_0' = E_0 \; \frac{a'}{a' \pm bTv} \; \frac{bRC_p \pm 1}{bRC_p}$$

Let B(t) be incremented at times $t = nT$ $(n=0,1,\ldots k,\ldots N)$ as in Fig. 6.9. Thus $C(t) = C_p(a \pm n)$ for $nT \leq t \leq (n+1)T$. Eqn. 6.1 becomes for the first half of the square wave input

$$\frac{dq}{dt} + \frac{q}{RC_p(a \pm n)} = \frac{E}{R} U_{-1}(t) \qquad nT \leq t \leq (n+1)T$$

The solution for $nT \leq t \leq (n+1)T$ and $t > 0$ corresponding to eqn. 6.3 is

$$e_0(t) = E\left[1 - \left(1 - \sum_{k=0}^{n-1} \frac{(a \pm k)}{(a \pm n)} e^{-\frac{T}{RC_p}\sum_{p=k+1}^{n-1}\frac{1}{a \pm p}} \left[1 - e^{-\frac{T}{RC_p(a \pm k)}}\right]\right) e^{-\frac{(t - nT)}{RC_p(a \pm n)}}\right] \tag{6.8}$$

During the second half of the square wave input eqn. 6.1 becomes

$$\frac{dq}{dt} + \frac{q}{RC_p(a' \pm n)} = 0 \qquad 0 \leq t \leq Tv$$

and the solution for $nT \leq t \leq (n+1)T$ corresponding to eqn. 6.7 is

$$e_0(t) = E_0\left(\frac{a' \; e^{-\frac{T}{RC_p}\sum_{k=0}^{n-1}\frac{1}{a' \pm k}}}{a' \pm n}\right) e^{-\frac{(t - nT)}{RC_p(a' \pm n)}} \qquad 0 \leq t \leq Tv \tag{6.9}$$

The details of the solution are omitted, as they are similar to those presented in conjunction with eqn. 5.17.

Eqns. 6.3 and 6.6 show that the general form of the output is greatly affected by the parameter bRC_p. Measured and calculated outputs were obtained for six different values of this parameter, the values being selected to show the various kinds of behaviour in $e_0(t)$. The outputs were calculated and plotted by an IBM 7040 computer for a and a' either 15 or 207, b = 192/msec, Tv = 1 msec and Tc = 1.5 msec, (See Fig. 6.11). The discrepancy in $e_0(t)$ for C(t) a continuous function and C(t) a stepwise approximation did not show on any of the plotted outputs. For this reason the calculated output $e_0(t)$ is shown only for C(t) continuous. The results in Figures 6.11 to 6.14 show photographs of the measured outputs and the corresponding calculated outputs. The close agreement between the calculated and measured results indicates the accuracy of the time-varying capacitor.

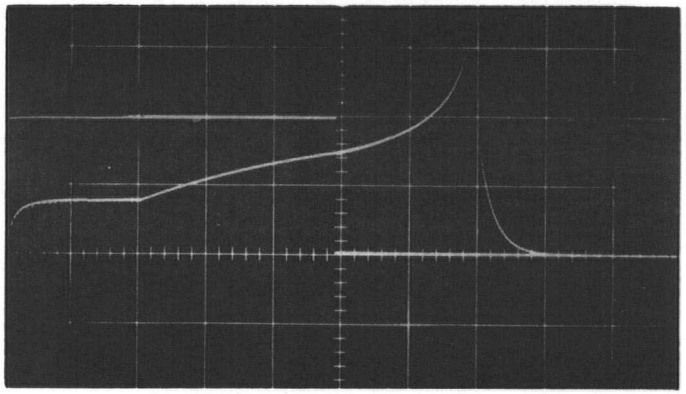

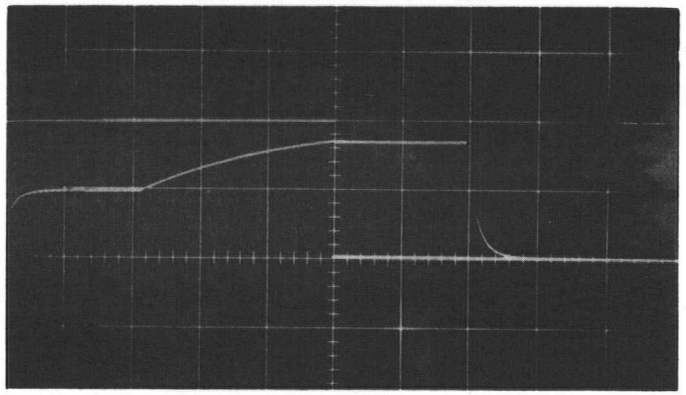

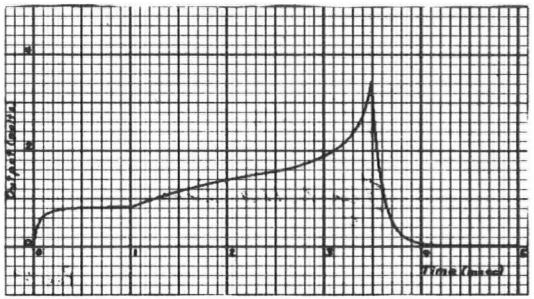

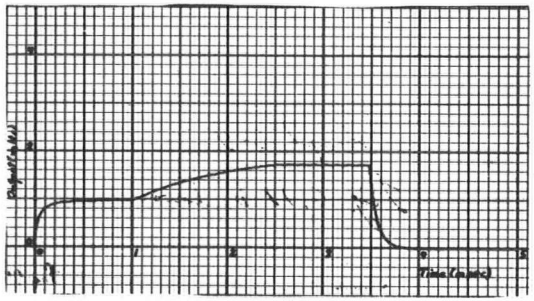

(a) (b)

Fig. 6.11 Calculated and Measured Output for R-C Circuit in Fig. 6.7 and Case 1 of Fig. 6.9. Upper Photographs: Vertical Scale; 1 volt/div. Horizontal Scale; 0.5 msec/div. Lower Graphs: Calculated Outputs. (a) $bRC_p = 1.43$ (b) $bRC_p = 1$.

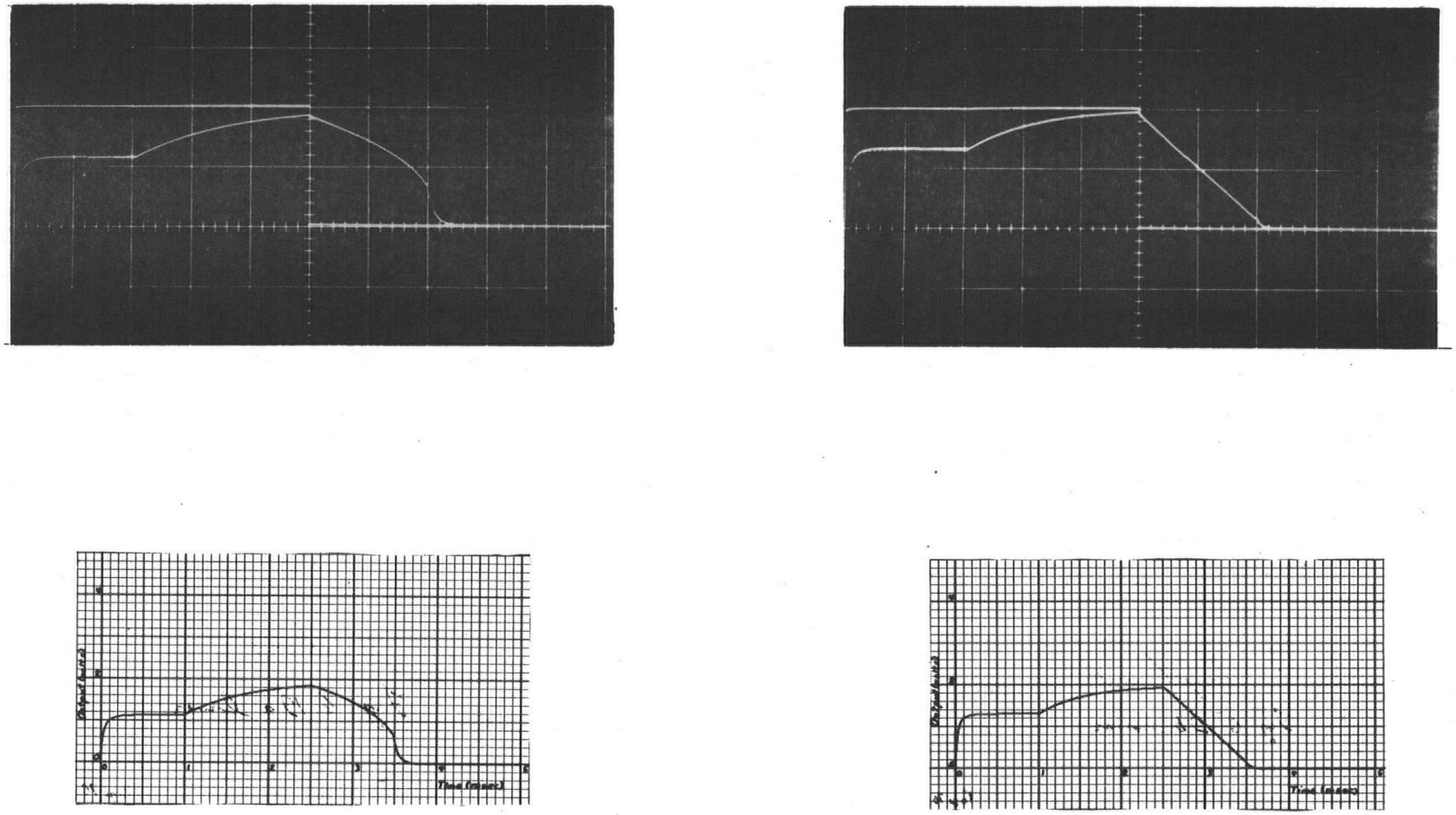

(a) (b)

Fig. 6.12 Calculated and Measured Output for R-C Circuit in Fig. 6.7 and Case 1 of Fig. 6.9. Upper Photographs: Vertical Scale; 1 volt/div, Horizontal Scale; 0.5 msec/div. Lower Graphs: Calculated Outputs. (a) $bRC_p = 0.714$ (b) $bRC_p = 0.5$.

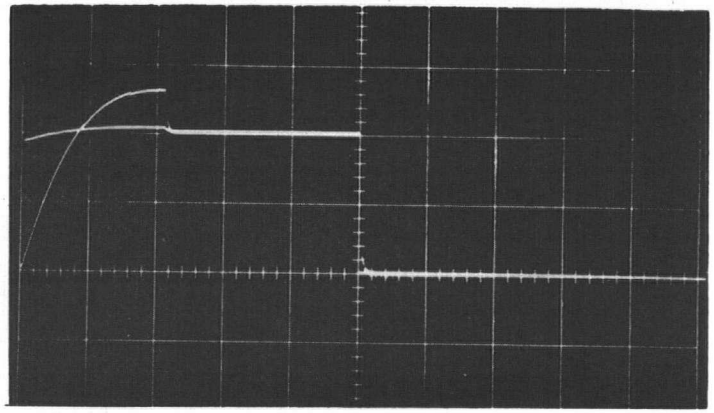

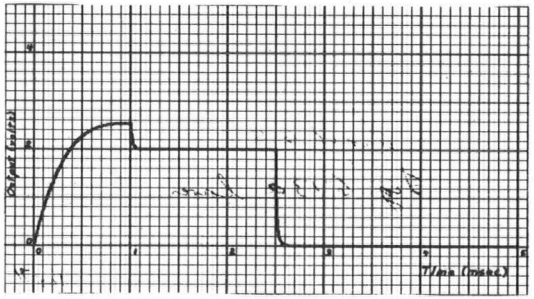

(a)

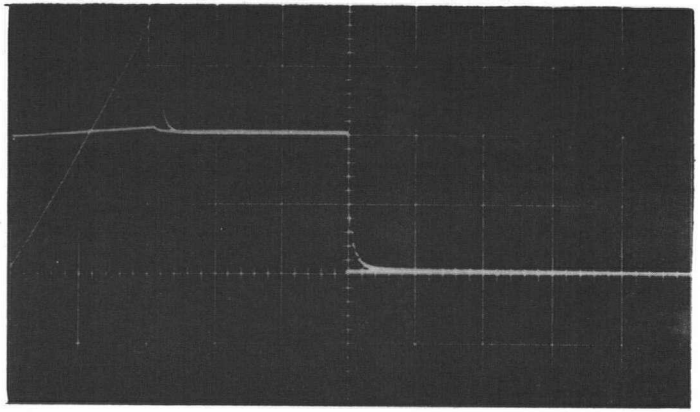

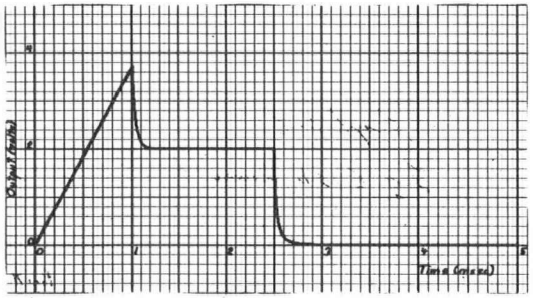

(b)

Fig. 6.13 Calculated and Measured Output for R-C Circuit in Fig. 6.7 and Case 2 of Fig. 6.9. Upper Photographs: Vertical Scale; 1 volt/div, Horizontal Scale; 0.5 msec/div. Lower Graphs: Calculated Outputs. (a) $bRC_p = 0.214$ (b) $bRC_p = 0.5$.

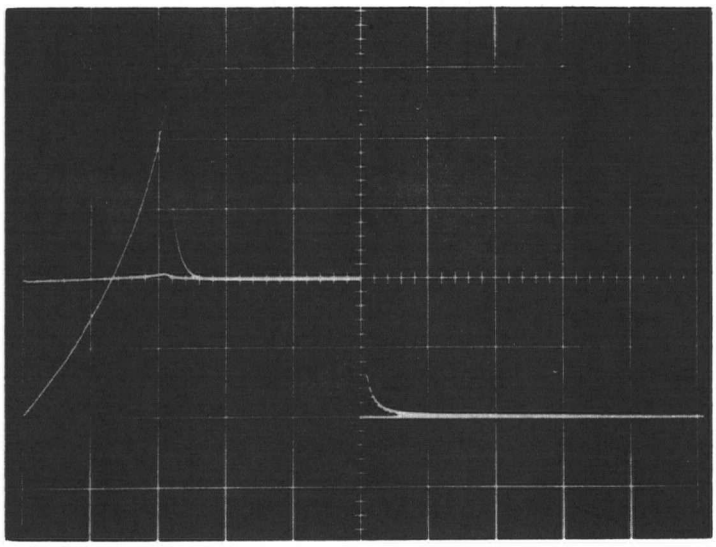

(a)

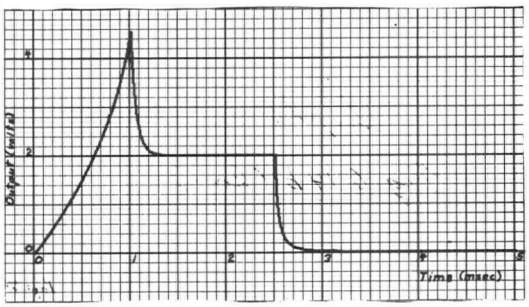

(b)

Fig. 6.14 Calculated and Measured Output for R-C Circuit in Fig. 6.7 and Case 2 of Fig. 6.9. $bRC_p = 0.714$. (a) Measured Output Vertical Scale; 1 volt/div, Horizontal scale; 0.5 msec/div. (b) Calculated Output.

REFERENCES

1. H.F. Olson, H. Belar and E.S. Rogers, Speech Processing Techniques and Applications, IEEE Trans. on Audio and Electroacoustics, Vol. AU-15, No. 3, Sept. 1967, pp. 120-126.

2. B. Gold, C.M. Rader, Systems for Compressing the Bandwidth of Speech, IEEE Trans. on Audio and Electroacoustics, Vol. AU-15, No. 3, Sept. 1967, pp. 131-136.

3. H.W. Dudley, Synthesizing Speech, Bell Labs. Record, Vol. 15, No. 4, Dec. 1936, pp. 98-102.

4. H.W. Dudley, The Carrier Nature of Speech, Bell System Tech. J., Vol. 19, No. 4, Oct. 1940, pp. 495-515.

5. M.R. Schroeder, Vocoders: Analysis and Synthesis of Speech, Proc. IEEE Vol. 54, No. 5, May 1966, pp. 720-734.

6. R.S. Tomlinson, The Design of a Digitally Controlled Attenuator, Quarterly Progress Report No. 74, Research Lab. of Electronics, M.I.T., July 15, 1964, pp. 185-190.

7. R.S. Tomlinson, SPASS - An Improved Terminal Analog Speech Synthesizer Quarterly Progress Report No. 80, Research Lab. of Electronics, M.I.T., Jan. 15, 1966, pp. 198-205.

8. J.L. Flanagan, Speech Analysis Synthesis and Perception, (New York: Academic Press Inc., 1965) pp. 21-74.

9. K.N. Stevens, S. Kasowski and C.G.M. Fant, An Electrical Analog of the Vocal Tract, J. Acoust. Soc. of Am., Vol. 25, No. 4, July 1953, pp. 734-742.

10. H.K. Dunn, The Calculation of Vowel Resonances, and an Electrical Vocal Tract, J. Acoust. Soc. of Am., Vol. 22, N.6, Nov. 1950, pp. 740-753.

11. G. Rosen, Dynamic Analog Speech Synthesizer, Technical Report 353, Research Lab. of Electronics, M.I.T., Feb. 10, 1960.

12. G. Rosen, Dynamic Analog Speech Synthesizer, J. Acoust. Soc. of Am., Vol. 30, No. 3, Mar. 1958, pp. 201-209.

13. M.H.L. Hecker, A.S. House and K.N. Stevens, Performance of the Articulatory Analog of the Speech Mechanism: A Report on the Status of Research, Quarterly Progress Report No. 64, Research Lab. of Electronics, M.I.T., Jan. 15, 1962, pp. 191-198.

14. J.B. Dennis, Speech Synthesis, Quarterly Progress Report No. 67, Research Lab. of Electronics, M.I.T., Oct. 15, 1962, pp. 157-162.

15. J.E. Fulenwider, High Q Inductance Simulation, Proc. IRE, Vol. 48, May 1960, pp. 954-955.

16. Y. Kanai, On the Inductive Part in the A.C. Characteristics of the Semiconductor Diodes, J. Phys. Soc., Japan, Vol. 10, 1955, pp. 719-720.

17. I. Ladany and R.J. Kearney, A High-Q tuned Circuit using a Solid-State Inductance, J. Electronics and Control, Vol. 10, Mar. 1961, pp. 241-243.

18. T. Chiba and M. Kajiyama, The Vowel, Its Nature and Structure, Phonetic Society of Japan, Tokyo, 1950, p. 121.

19. Flanagan, op. cit., pp. 14-21.

20. R.K. Potter, G.A. Kopp and H.C. Green, Visible Speech, D. Van Nostrand Company, Inc., 1947.

21. R.H.S. Riordan, Simulated Inductors using Differential Amplifiers, Electronics Letters, Vol. 3, No. 2, Feb. 1967, pp. 50-51.

22. G. Austin, Design and Construction of an Opaque Optical Contour Tracer for Character Recognition Research, M.A.Sc. Thesis, Department of Electrical Engineering, U.B.C., 1968.

23. E.D. Rainville, A Short Course in Differential Equations, (New York: Macmillan Comp., 2nd Ed., 1961).